



Published in final edited form as:

Cell Rep. 2021 June 08; 35(10): 109227. doi:10.1016/j.celrep.2021.109227.

## Ontogenic timing, T cell receptor signal strength, and Notch signaling direct $\gamma\delta$ T cell functional differentiation *in vivo*

Edward L.Y. Chen<sup>1,2</sup>, Christina R. Lee<sup>1</sup>, Patrycja K. Thompson<sup>1</sup>, David L. Wiest<sup>3</sup>, Michele K. Anderson<sup>1,2</sup>, Juan Carlos Zúñiga-Pflücker<sup>1,2,4,\*</sup>

<sup>1</sup>Sunnybrook Research Institute, Toronto, ON, Canada

<sup>2</sup>Department of Immunology, University of Toronto, Toronto, ON, Canada

<sup>3</sup>Blood Cell Development and Function, Fox Chase Cancer Center, Philadelphia, PA, USA

<sup>4</sup>Lead contact

### SUMMARY

$\gamma\delta$  T cells form an integral arm of the immune system and are critical during protective and destructive immunity. However, how  $\gamma\delta$  T cells are functionally programmed *in vivo* remains unclear. Here, we employ RBPJ-inducible and KN6-transgenic mice to assess the roles of ontogenic timing, T cell receptor (TCR) signal strength, and Notch signaling. We find skewing of  $V\gamma 1^+$  cells toward the PLZF<sup>+</sup>Lin28b<sup>+</sup> lineage at the fetal stage. Generation of interleukin-17 (IL-17)-producing  $\gamma\delta$  T cells is favored during, although not exclusive to, the fetal stage. Surprisingly, Notch signaling is dispensable for peripheral  $\gamma\delta$  T cell IL-17 production. Strong TCR signals, together with Notch, promote IL-4 differentiation. Conversely, less strong TCR signals promote Notch-independent IL-17 differentiation. Single-cell transcriptomic analysis reveals differential programming instilled by TCR signal strength and Notch for specific subsets. Thus, our results precisely define the roles of ontogenic timing, TCR signal strength, and Notch signaling in  $\gamma\delta$  T cell functional programming *in vivo*.

### In brief

Ontogeny and TCR signal strength are known to influence  $\gamma\delta$  T cell differentiation. Chen et al. show that temporal control of Notch signaling in RBPJ-inducible mice affects innate  $\gamma\delta$  T cell differentiation. TCR signal strength and Notch influence IL-4 versus IL-17  $\gamma\delta$  T cell programming, which correlate with low versus high *Ccr9* expression, respectively.

This is an open access article under the CC BY-NC-ND license (<http://creativecommons.org/licenses/by-nc-nd/4.0/>).

\*Correspondence: jczp@sri.utoronto.ca.

#### AUTHOR CONTRIBUTIONS

E.L.Y.C. designed and performed experiments, analyzed the data, and wrote the manuscript. C.R.L. provided technical assistance. P.K.T. generated the RBPJ<sup>ind</sup> mice. D.L.W. provided the KN6<sup>tg</sup> mice. M.K.A. designed experiments, analyzed the data, and wrote the manuscript. J.C.Z.-P. designed experiments, analyzed the data, and wrote the manuscript.

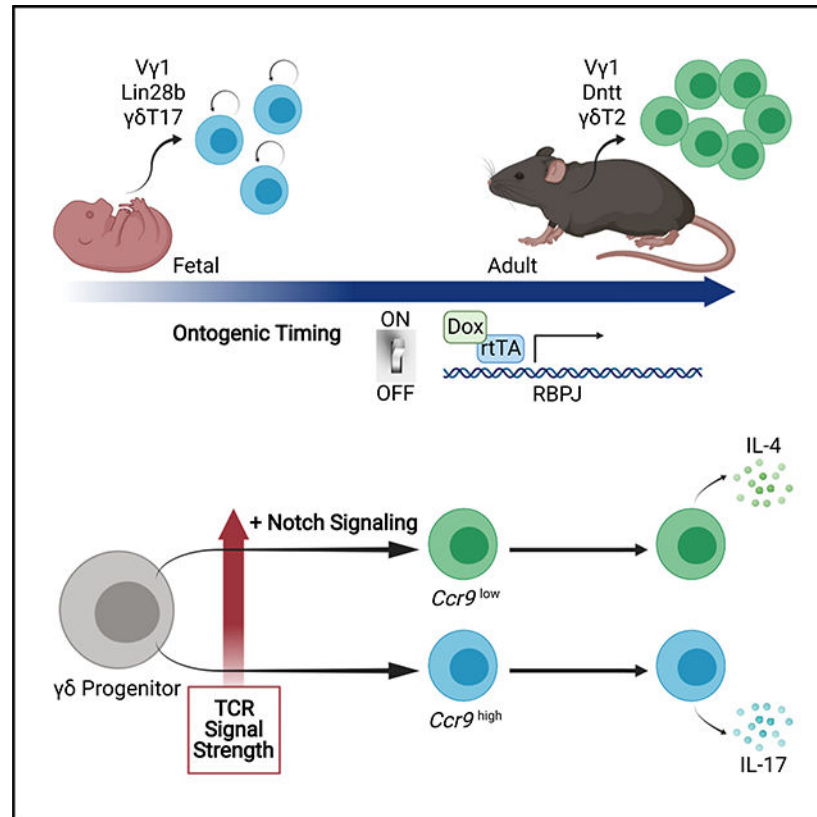
#### DECLARATION OF INTERESTS

J.C.Z.-P. is a co-founder and chair of the Scientific Advisory Board of Notch Therapeutics.

#### SUPPLEMENTAL INFORMATION

Supplemental information can be found online at <https://doi.org/10.1016/j.celrep.2021.109227>.

## Graphical Abstract



## INTRODUCTION

T cell commitment occurs at the  $CD4^-CD8^-$  double-negative (DN) 3 stage of T cell development, when cells bifurcate into the  $\alpha\beta$  or  $\gamma\delta$  lineage (Ciofani et al., 2006; Wong and Zúñiga-Pflücker, 2010). Both T cell lineages can secrete interferon  $\gamma$  ( $IFN\gamma$ ), interleukin-4 (IL-4), or IL-17 (In et al., 2017; Parker and Ciofani, 2020; Zarin et al., 2015). However,  $\gamma\delta$  T cells are distinct in that ontogenic timing is thought to influence the generation of specific  $V\gamma$  repertoires and functional subsets (Carding and Egan, 2002; Prinz et al., 2013). Additionally, although functional differentiation of  $\alpha\beta$  T cells typically occurs in the periphery,  $\gamma\delta$  T cells may acquire their functional fates during intrathymic development (In et al., 2017; Parker and Ciofani, 2020; Zarin et al., 2015). The roles of ontogenic timing, T cell receptor (TCR) signal strength, and Notch signaling in  $\gamma\delta$  T cell functional programming *in vivo* remain to be fully elucidated.

The ability of  $\gamma\delta$  T cells to secrete cytokines at faster “innate-like” kinetics distinguishes them from “adaptive”  $\alpha\beta$  T cells (Schmolka et al., 2015; Vantourout and Hayday, 2013). Innate-like  $\gamma\delta$  T cells comprise  $V\gamma 1^+$  promyelocytic leukemia zinc-finger-positive (PLZF<sup>+</sup>) cells, which include IL-4-producing ( $\gamma\delta T2$ ) and IL-17-producing ( $\gamma\delta T17$ ) cells (Akitsu and Iwakura, 2018; Alonzo et al., 2010; Kreslavsky et al., 2009; Papotto et al., 2017b). There is controversy regarding  $\gamma\delta T17$  generation, because there are conflicting reports as to whether

these cells are exclusively made fetally (Gray et al., 2013; Haas et al., 2012; Kashani et al., 2015; Papotto et al., 2017a). The roles of TCR and Notch signaling in mediating  $\alpha\beta$  versus  $\gamma\delta$  lineage decisions are well understood (Ciofani et al., 2006; Lauritsen et al., 2009). However, it remains to be resolved whether these factors dictate  $\gamma\delta$  T cell functional programming *in vivo*. Deficiency in inhibitor of DNA binding (ID) 3, which is downstream of TCR signaling, results in expansion of  $V\gamma 1^{+}PLZF^{+}$  cells (Alonzo et al., 2010; Lauritsen et al., 2009). However, the TCR signal strength needed for  $\gamma\delta T2$  generation, along with the role for Notch, requires further examination. Additionally,  $\gamma\delta T17$  generation has been shown to require weaker TCR signals and Notch *in vitro* (Zarin et al., 2018). However, whether this is consistent *in vivo* remains to be investigated.

Here, we used RBPJ-inducible (RBPJ<sup>ind</sup>) mice in which Notch responsiveness, and thus T cell development (Chen et al., 2019), can be restricted to fetal, neonatal, or adult periods. We found that the fetal period generated fewer  $V\gamma 1^{+}$  cells, but these  $V\gamma 1^{+}$  cells were enriched for PLZF and Lin28b expression. The fetal period was favorable for  $\gamma\delta T17$  generation, but lung  $\gamma\delta T17$  cells could still be made post-natally. However, only fetal-derived lung  $\gamma\delta T17$  cells possessed innate  $\gamma\delta T17$  functionality, which, contrary to previous reports (Nakamura et al., 2015; Shibata et al., 2011), was Notch independent. Using KN6  $\gamma\delta TCR$ -transgenic (KN6<sup>tg</sup>) mice (in which  $\gamma\delta TCR$  signal strength can be modulated), RBPJ<sup>ind</sup>KN6<sup>tg</sup> mice, and single-cell RNA sequencing (scRNA-seq) analysis, we found that strong TCR signals and Notch promoted  $\gamma\delta T2$  development. Conversely, less strong TCR signals favored  $\gamma\delta T17$  development, which was Notch independent. Altogether, these results reveal the precise roles of ontogenic timing, TCR signal strength, and Notch signaling in  $\gamma\delta$  T cell functional programming *in vivo*.

## RESULTS

### Fetal-, neonatal-, and adult-specific T cell development in RBPJ<sup>ind</sup> mice

RBPJ<sup>ind</sup> mice, in which doxycycline (Dox) induces expression of an RBPJ transgene, allow for temporal control of T cell development, as previously described (Chen et al., 2019). Here, we restricted T cell development to fetal, neonatal, or adult periods to assess the role of ontogeny in  $\gamma\delta$  T cell differentiation. For fetal-specific induction, pregnant mice were Dox treated from conception to birth; for neonatal-specific induction, nursing mice were Dox treated from birth to 3 weeks of age; and for adult-specific induction, mice were Dox treated from 6 to 9 weeks of age (Figure S1A). Thymi from Dox-untreated RBPJ<sup>ind</sup> mice (-Dox) at embryonic day (E) 16, neonatal day 12, and adult day 54 displayed a block at the CD44<sup>+</sup>CD25<sup>-</sup> DN1 stage and absence of CD3<sup>+</sup> $\gamma\delta TCR^{+}$  cells (Figure S1B). In contrast, thymi from Dox-treated RBPJ<sup>ind</sup> mice (+Dox) showed CD44<sup>+</sup>CD25<sup>+</sup> DN2, CD44<sup>-</sup>CD25<sup>+</sup> DN3, and CD44<sup>-</sup>CD25<sup>-</sup> DN4 cells and the presence of CD3<sup>+</sup> $\gamma\delta TCR^{+}$  cells (Figure S1B). These results demonstrate that  $\gamma\delta$  T cell development can be temporally regulated in a tight fashion in RBPJ<sup>ind</sup> mice.

Fetal induction of T cell development led to the generation of several  $V\gamma$  subsets in the RBPJ<sup>ind</sup> fetal thymus.  $V\gamma 5^{+}$  cells (Tonegawa nomenclature; Heilig and Tonegawa, 1986) were the major  $\gamma\delta$  T cell population from E16 to E17, and  $V\gamma 4^{+}$  cells were the major population from E20 to E21, while  $V\gamma 1^{+}$  and  $V\gamma 7^{+}$  cells were a small proportion

throughout (Figure S1C). Adult induction of T cell development led to the generation of  $V\gamma 1^+$ ,  $V\gamma 4^+$ , and  $V\gamma 7^+$ , but not  $V\gamma 5^+$ , cells in the RBPJ<sup>ind</sup> adult thymus.  $V\gamma 4^+$  cells were the major  $\gamma\delta$  T cell population during the first 4 days, and  $V\gamma 1^+$  cells were the major population from day 5 onward, while  $V\gamma 7^+$  cells were a small proportion throughout (Figure S1C). These results are consistent with previous reports showing fetal-exclusive  $V\gamma 5$  generation (Havran and Allison, 1990; Ikuta et al., 1990), demonstrating that RBPJ<sup>ind</sup> mice reflect physiological outcomes. Additionally, our findings show that the fetal period biases toward  $V\gamma 4$  generation, while the adult period biases toward  $V\gamma 1$  generation.

The periphery was analyzed in 12-week-old RBPJ<sup>ind</sup> mice following fetal, neonatal, or adult induction of T cell development. Dox-untreated RBPJ<sup>ind</sup> mice displayed no  $CD3^+$  T cells in spleen and lymph nodes, while fetal-, neonatal-, and adult-induced mice showed the appearance of  $\gamma\delta$  T cells (Figure S1D). Fetal-induced mice contained  $CD3^{\text{hi}}\gamma\delta\text{TCR}^{\text{hi}}V\gamma 5^+$  cells in the epidermis, while post-natal-induced mice did not (Figure 1A). Fetal-induced mice contained  $V\gamma 6^+$  cells in the lung, while post-natal-induced mice contained very few to none (Figure 1A). Fetal- and neonatal-induced mice showed similar percentages of  $V\gamma 7^+$  cells among intestinal epithelial  $\gamma\delta$  T cells, with adult-induced mice showing a slight reduction (Figure 1A). Fetal-induced mice contained very few  $V\gamma 1^+$  cells in spleen and lymph nodes, which predominantly consisted of  $V\gamma 4^+$  cells (Figure 1B). Conversely, in post-natal-induced mice,  $V\gamma 1^+$  cells were the predominant  $\gamma\delta$  T cell population, while  $V\gamma 4^+$  cells were reduced in percentage by about 3-fold (Figure 1B). These data provide additional evidence for fetal-exclusive  $V\gamma 5$  and  $V\gamma 6$  generation (Cai et al., 2014; Havran and Allison, 1990; Ikuta et al., 1990; Nitta et al., 2015) and show predominant development of  $V\gamma 4$  fetally, but predominant development of  $V\gamma 1$  post-natally.

### Fetal-derived $V\gamma 1^+$ cells are enriched for PLZF and Lin28b expression

$V\gamma 1^+$  cells expressing PLZF are thought to be  $\gamma\delta$  natural killer (NK) T (NKT) cells (Alonzo et al., 2010; Kreslavsky et al., 2009). Fetal-, neonatal-, and adult-derived  $V\gamma 1^+$  cells were further analyzed for PLZF expression. In thymus and spleen, ~50% and ~40% of fetal-derived  $V\gamma 1^+$  cells were PLZF<sup>+</sup>, respectively (Figure 1C). In comparison, the PLZF<sup>+</sup> percentage was reduced 2-fold and 6- to 8-fold in post-natal-derived  $V\gamma 1^+$  cells, respectively (Figure 1C). Total cell numbers showed that fetal, neonatal, and adult periods produced similar quantities of  $V\gamma 1^+$ PLZF<sup>+</sup> cells (Figure 1C), suggesting that although the fetal period generates fewer  $V\gamma 1^+$  cells, on a per-cell basis, it is more permissive for  $V\gamma 1^+$  cell differentiation toward the  $\gamma\delta$  NKT cell lineage.

To further elucidate the role of ontogeny in  $V\gamma 1^+$  cell development, we performed RNA sequencing (RNA-seq) on mature  $CD24^-$  fetal (from RBPJ-sufficient newborn thymi) and adult (from adult-induced RBPJ<sup>ind</sup> adult thymi)  $V\gamma 1^+$  cells. Differential expression analysis revealed that many genes were upregulated in fetal or adult  $V\gamma 1^+$  cells, compared with each other, of which 985 and 803 genes were significant, respectively (Figure 2A; Table S1). Notably, fetal  $V\gamma 1^+$  cells displayed the Lin28b<sup>+</sup> gene signature (*Lin28b*, *Arid3a*, *Igf2*, and *Igf2bp3*) that was lost in adult  $V\gamma 1^+$  cells, a feature that endows fetal hematopoiesis properties, including innateness (Yuan et al., 2012) (Figure 2B; Table S1). Adult  $V\gamma 1^+$  cells instead had high expression of adaptive immunity genes, such as *Dntt*, which permits TCR

diversity (Aono et al., 2000), and *Sell*, which is expressed by naive T cells (Prinz et al., 2013) (Figure 2B; Table S1). Interestingly, while Lin28b was enriched in fetal V $\gamma$ 1<sup>+</sup> cells (which correlates with their skewing toward the  $\gamma\delta$  NKT cell lineage), adult V $\gamma$ 1<sup>+</sup> cells displayed  $\gamma\delta$ T1/2-like features. Fetal V $\gamma$ 1<sup>+</sup> cells showed enriched expression of  $\gamma\delta$ T17 genes, *Blk*, *Il17a*, and *Il17f* (Laird et al., 2010), while adult V $\gamma$ 1<sup>+</sup> cells had enriched expression of  $\gamma\delta$ T1 genes, *Slamf6* and *Ifng* (Dienz et al., 2020), and  $\gamma\delta$ T2 genes, *Cd4* and *Il4* (Alonzo et al., 2010) (Figure 2B; Table S1). This suggests that IL-17 potential is instilled in fetal V $\gamma$ 1<sup>+</sup> cells, while adult V $\gamma$ 1<sup>+</sup> cells are poised for IFN $\gamma$  and IL-4 production.

The Lin28b program also promotes proliferation and self-renewal/survival (Xu et al., 2020). This was also observed in fetal V $\gamma$ 1<sup>+</sup> cells that showed upregulated expression of *Cdk* and *Ccn* cell-cycle genes compared with adult V $\gamma$ 1<sup>+</sup> cells (Figure 2B; Table S1). Fetal V $\gamma$ 1<sup>+</sup> cells also had higher expression of Notch pathway genes, *Notch3* and *Nrarp* (Figure 2B; Table S1). Together with Lin28b, Notch signaling can promote the observed increased expression of proliferation genes, *Myc* and *Mycn* (Weng et al., 2006; Xu et al., 2020) (Figure 2B; Table S1). Additionally, fetal V $\gamma$ 1<sup>+</sup> cells showed upregulation of self-renewal/survival genes, *Akt1* and *Birc5* (Xu et al., 2020), while adult V $\gamma$ 1<sup>+</sup> cells showed upregulation of quiescence genes, *Btg1* and *Btg2* (Hwang et al., 2020) (Figure 2B; Table S1). Other functional properties that distinguished fetal and adult V $\gamma$ 1<sup>+</sup> cells include the expression of *Gzm* and *Ifitm* genes, which confers resistance to viral infections (Wakim et al., 2013), in fetal cells, and the expression of *Tlr* and *Klra* genes, which function as NK inhibitory receptors (Schenkel et al., 2013), in adult cells (Figure 2B; Table S1). Altogether, these results suggest that fetal context is necessary for induction of Lin28b, which promotes innateness in fetal V $\gamma$ 1<sup>+</sup> cells and endows them with specific functional assets and cell maintenance strategies that are distinct from adult V $\gamma$ 1<sup>+</sup> cells.

### The fetal period is favorable, but not exclusive, for $\gamma\delta$ T17 generation

Lymph nodes and lung from fetal-, neonatal-, and adult-induced RBPJ<sup>ind</sup> mice were analyzed for CD27 expression in  $\gamma\delta$  T cells, because CD27<sup>+</sup> correlates with IFN $\gamma$  producers ( $\gamma\delta$ T1) and CD27<sup>-</sup> correlates with  $\gamma\delta$ T17 cells (Ribot et al., 2009; Schmolka et al., 2013). Fetal-derived lymph node  $\gamma\delta$  T cells contained equal proportions of CD27<sup>+</sup> and CD27<sup>-</sup> cells (Figure 3A). The CD27<sup>-</sup> population was greatly reduced in post-natal-derived lymph node  $\gamma\delta$  T cells (Figure 3A). In contrast, nearly all post-natal-derived lung  $\gamma\delta$  T cells were CD27<sup>-</sup>, comparable with fetal-derived cells (Figure 3A).  $\gamma\delta$  T cells were stimulated *in vitro* with phorbol 12-myristate 13-acetate (PMA) and ionomycin to determine their IL-17-producing capacity. Fetal-derived lymph node  $\gamma\delta$  T cells were capable of IL-17 production, in stark contrast with the near absence of lymph node  $\gamma\delta$ T17 cells in post-natal-induced mice (Figure 3B). Surprisingly, fetal-, neonatal-, and adult-derived lung  $\gamma\delta$  T cells were all capable of IL-17 production, albeit with post-natal-induced mice showing a lower frequency of lung  $\gamma\delta$ T17 cells (Figure 3B). Adult-derived lung  $\gamma\delta$ T17 cells consisted of V $\gamma$ 1<sup>+</sup> and V $\gamma$ 4<sup>+</sup> cells (Figure S2A). These results suggest that the fetal period provides a more permissive environment for  $\gamma\delta$ T17 generation. However, the strict requirement for fetal timing for IL-17 differentiation does not apply for certain tissue-specific  $\gamma\delta$  T cells.

## Peripheral $\gamma\delta$ T17 function is Notch independent

Conditional deletion of *Hes1* in peripheral  $\gamma\delta$  T cells was shown to impair IL-17 production, suggesting that Notch is critical for peripheral  $\gamma\delta$ T17 function (Nakamura et al., 2015; Shibata et al., 2011). We wanted to extend these findings by investigating whether controlling Notch responsiveness affected lung  $\gamma\delta$ T17 function in response to an inflammatory challenge. We employed trehalose dimycolate (TDM) to mimic *M. tuberculosis* infection, because it activates Mincle receptors on monocytes to produce IL-1 $\beta$  and IL-23, which in turn stimulate  $\gamma\delta$  T cells to produce IL-17 (Saitoh et al., 2012). Consistently, compared with mock-injected mice, TDM-injected mice showed increased lung  $\gamma\delta$  T cell IL-17 production (Figure S2B).

To determine the ability of fetal- and adult-derived lung  $\gamma\delta$  T cells to produce IL-17 in response to TDM in the absence or presence of Notch signaling, fetal- or adult-induced RBPJ<sup>ind</sup> mice remained Dox untreated (-Dox) or were Dox treated (+Dox) for 1 week and were exposed to TDM for 2 days prior to analysis (Figure S2C). In control (RBPJ-sufficient) mice, lung  $\gamma\delta$  T cells displayed a strong IL-17 response, whereas lung  $\alpha\beta$  T cells did not, demonstrating innate-specific reactivity (Figure 3C). In fetal-induced -Dox mice, the total number of IL-17<sup>+</sup> lung  $\gamma\delta$  T cells was similar to control mice (Figure 3C; Figure S2D). In contrast with control and fetal-induced -Dox, adult-induced -Dox lung  $\gamma\delta$  T cells did not display an IL-17 response (Figure 3C; Figure S2D). This suggests that although adult-derived  $\gamma\delta$  T cells possess IL-17-producing capacity, it is not through an innate-like fashion. When Notch responsiveness was re-initiated in fetal-induced +Dox and adult-induced +Dox mice, the total number of IL-17<sup>+</sup> lung  $\gamma\delta$  T cells was unchanged compared with -Dox conditions (Figure 3C; Figure S2D). This suggests that peripheral  $\gamma\delta$ T17 function of fetal-derived  $\gamma\delta$  T cells can proceed without Notch signaling.

## Generation of KN6<sup>tg</sup> and RBPJ<sup>ind</sup>KN6<sup>tg</sup> mice

To investigate TCR and Notch signaling in  $\gamma\delta$  T cell functional programming, we bred RBPJ<sup>ind</sup> mice (B6; H-2T<sup>b/b</sup>) to recombination activating gene 2 (RAG2)-deficient KN6<sup>tg</sup> mice (BALB/c; H-2T<sup>d/d</sup>). This generated KN6<sup>tg</sup> mice (H-2T<sup>b/d</sup>/H-2T<sup>d/d</sup>) to study TCR signal strength and RBPJ<sup>ind</sup>KN6<sup>tg</sup> mice (H-2T<sup>b/d</sup>/H-2T<sup>d/d</sup>) to study TCR signal strength with Notch (Figure S3A). The KN6  $\gamma\delta$ TCR (V $\gamma$ 4V $\delta$ 5) recognizes non-classical MHC Ib molecules T10 and T22 but binds T22 at a 10-fold higher affinity compared with T10 (Adams et al., 2008; Ito et al., 1990). The H-2T<sup>b</sup> allele contains functional T10 and T22, but the H-2T<sup>d</sup> allele contains functional T10 only (Adams et al., 2008; Ito et al., 1990). Thus, the H-2T<sup>b</sup> allele provides a strong ligand for KN6, while the H-2T<sup>d</sup> allele provides a less strong ligand for KN6. Consistently, when analyzing 10-week-old KN6<sup>tg</sup> mice, thymic KN6 cells of H-2T<sup>b/d</sup> mice (b/d; strong) displayed a lower CD3 mean fluorescence intensity (MFI) compared with thymic KN6 cells of H-2T<sup>d/d</sup> mice (d/d; less strong) (Bendelac et al., 2007) (Figure S3B). CD24 and CD73 were then analyzed, in which gaining CD73 expression marks  $\gamma\delta$  lineage commitment and losing CD24 expression marks  $\gamma\delta$  lineage maturation (Coffey et al., 2014; Fahl et al., 2018). In the b/d thymus, few KN6 cells were CD24<sup>+</sup>CD73<sup>-</sup> and many were CD24<sup>+</sup>CD73<sup>hi</sup>, CD24<sup>-</sup>CD73<sup>hi</sup>, or CD24<sup>-</sup>CD73<sup>lo</sup> (Figure S3C). Conversely, in the d/d thymus, many KN6 cells were CD24<sup>+</sup>CD73<sup>-</sup>, few were

CD24<sup>+</sup>CD73<sup>hi</sup>, and appreciable CD24<sup>-</sup>CD73<sup>hi</sup> and CD24<sup>-</sup>CD73<sup>lo</sup> cells were present (Figure S3C).

### Strong TCR signals promote $\gamma\delta$ T2 generation

Thymocytes from b/d and d/d KN6<sup>tg</sup> mice were stimulated *in vitro* with PMA and ionomycin to determine their functional capacities. KN6 cells from both mice robustly produced IFN $\gamma$  and did not display major differences in  $\gamma\delta$ T1 percentage and number (Figure S4A). CD24<sup>+</sup>CD73<sup>-</sup>, CD24<sup>+</sup>CD73<sup>hi</sup>, CD24<sup>-</sup>CD73<sup>hi</sup>, and CD24<sup>-</sup>CD73<sup>lo</sup> populations from both mice produced IFN $\gamma$  (Figures 4A and 4B). Additionally, spleen, lymph node, and lung KN6 cells from both mice robustly produced IFN $\gamma$ , with b/d mice showing slightly higher  $\gamma\delta$ T1 percentages (Figure S4B). These results suggest that either strength of TCR signaling is permissive for  $\gamma\delta$ T1 differentiation (Jensen et al., 2008; Ribeiro et al., 2015).

Thymic KN6 cells from b/d mice displayed IL-4 functional capacity (about 4% of cells), while  $\gamma\delta$ T2 cells were virtually absent in d/d mice (Figure 4A). The percentage and number of total  $\gamma\delta$ T2 cells were significantly higher in b/d mice compared with d/d mice, and similarly when fractionating into IFN $\gamma$ <sup>-</sup>IL-4<sup>+</sup> and IFN $\gamma$ <sup>+</sup>IL-4<sup>+</sup> cells (Figure 4A).  $\gamma\delta$ T2 cells from b/d mice were found within CD24<sup>+</sup>CD73<sup>hi</sup> and CD24<sup>-</sup>CD73<sup>hi</sup> populations (Figure 4A). In spleen, there were appreciable IL-4<sup>+</sup> cells in b/d mice, which were virtually absent in d/d mice (Figure S4B). These results suggest that strong TCR signals promote  $\gamma\delta$ T2 (and thus  $\gamma\delta$  NKT cell) differentiation.

### Less strong TCR signals promote $\gamma\delta$ T17 generation

Thymic KN6 cells from both b/d and d/d mice displayed IL-17 functional capacity (Figure 4B). However, d/d mice showed greater  $\gamma\delta$ T17 generation, because the percentage and number of total  $\gamma\delta$ T17 cells were significantly higher compared with b/d mice (Figure 4B). When fractionating the IL-17<sup>+</sup> population, IFN $\gamma$ <sup>-</sup>IL-17<sup>+</sup> cells were higher in d/d mice, while IFN $\gamma$ <sup>+</sup>IL-17<sup>+</sup> cells were slightly higher in b/d mice (Figure 4B). The few  $\gamma\delta$ T17 cells from b/d mice were found within CD24<sup>+</sup>CD73<sup>hi</sup> and CD24<sup>-</sup>CD73<sup>hi</sup> populations, while  $\gamma\delta$ T17 cells from d/d mice were found within the CD24<sup>-</sup>CD73<sup>hi</sup> compartment (Figure 4B). Additionally, thymic KN6 cells from d/d mice were more potent IL-17 producers compared with b/d mice, as demonstrated by a significantly higher IL-17 MFI (Figure 4C). In spleen, lymph nodes, and lung, d/d mice showed higher percentages of KN6  $\gamma\delta$ T17 cells compared with b/d mice (Figure S4C). These results suggest that less strong TCR signals promote  $\gamma\delta$ T17 differentiation.

Thus far, IL-17-producing capabilities were assessed with PMA and ionomycin. Innate-like  $\gamma\delta$ T17 cells can also produce IL-17 in response to IL-1 $\beta$  and IL-23 (Chien et al., 2013; Jouan et al., 2018). No IL-17<sup>+</sup> thymic KN6 cells from b/d mice were detected with IL-1 $\beta$  and IL-23 stimulation, similar to unstimulated controls (Figure 4D). In contrast, IL-17<sup>+</sup> thymic KN6 cells from d/d mice were readily detected with IL-1 $\beta$  and IL-23 stimulation (Figure 4D). These data demonstrate that innate-like  $\gamma\delta$ T17 generation is fully dependent on less strong TCR signals.

## Transcriptomic analysis of b/d versus d/d thymic KN6 cells

To further elucidate the role of TCR signal strength in  $\gamma\delta$  T cell functional programming, we performed scRNA-seq on thymic KN6 cells from b/d and d/d KN6<sup>tg</sup> mice. In total, 2,112 b/d and 2,753 d/d cells were analyzed in which uniform manifold approximation and projection (UMAP) analysis revealed 12 clusters, of which clusters 1–8 contained substantial numbers (Figure 5A). Clusters 6 and 4 expressed proliferation genes and *Cd24a*, but not *Nt5e* (CD73), and thus are uncommitted  $\gamma\delta$  T cell progenitors (Figure 5A; Figure S5A; Table S2). Cluster 1 expressed *Nt5e* and *Sox4*, a key factor in  $\gamma\delta$  lineage differentiation (Melichar et al., 2007), but did not express functional-specific genes, and thus are committed  $\gamma\delta$  T cell progenitors (Figure 5A; Figure S5A; Table S2). Cluster 7 expressed genes that have not been characterized in the context of  $\gamma\delta$  T cells but included *Tnfrsf9* (4–1BB), *Ncl*, and *Xcl1* (Figure 5A; Table S2). Cluster 5 expressed intraepithelial lymphocyte (IEL) genes, such as *Cd8a*, *Itgae*, and *Itgal* (Sheridan and Lefrançois, 2010) (Figure 5A; Table S2). Cluster 2 expressed NK genes, such as *Klrk1*, *Klrd1*, and *Klrc1* (Crinier et al., 2018) (Figure 5A; Table S2). Cluster 3 did not express functional-specific genes but based on their separation from cluster 1, they are likely mature naive  $\gamma\delta$  T cells and are defined by *Dap11*, *Ly6c2*, and *Gm12840* (Figure 5A; Table S2). Cluster 8 expressed innate  $\gamma\delta$ T17 genes, such as *Blk*, *Maf*, *Rorc*, *Ccr6*, *Il1r1*, and *Il23r* (Zuberbuehler et al., 2019) (Figure 5A; Table S2). A full transcriptomic analysis at single-cell resolution revealed additional genes that further define each functional subset (Table S2).

By partitioning the UMAP and comparing b/d versus d/d cell numbers in each cluster, it revealed that d/d contained more cluster 6 and 4 cells, as expected given the role of TCR signaling in  $\gamma\delta$  lineage commitment (Figure 5A). Moreover, d/d contained more cluster 1 cells, which showed a clear UMAP separation from b/d cluster 1 cells (Figure 5A). In contrast, b/d contained more cluster 7, 5, and 2 cells (Figure 5A), further exemplifying that strong TCR signals enable  $\gamma\delta$  NKT cell programming, and that it enhances IEL generation. Meanwhile, d/d contained more cluster 3 and 8 cells (Figure 5A), further exemplifying that less strong TCR signals enable innate  $\gamma\delta$ T17 programming, and that it enhances naive  $\gamma\delta$  T cell generation. The distribution of b/d versus d/d cells to these clusters is significantly different (Table S3).

We next performed pseudotime analysis to predict cell trajectories (Cao et al., 2019). Starting from cluster 6, b/d KN6 cells can proceed to cluster 7 or cluster 1 (Figure 5B). Proceeding to cluster 1 appears to enable further differentiation to cluster 5, or even further differentiation to cluster 2 (Figure 5B). Starting from cluster 6, d/d KN6 cells appear to proceed to cluster 1 and then to cluster 3, where a few cells may differentiate to cluster 5 or cluster 2 (Figure 5B). A cell trajectory to cluster 8 could not be constructed because of a lack of intermediate cells, but cluster 8 is likely preceded by the rightmost cluster 1 cells (Figure 5B). The clear UMAP separation of b/d and d/d cluster 1 cells and the alternative paths they take for their functional differentiation led us to probe for differentially expressed genes that may explain these differences. Notably, b/d cells differentiated toward cluster 1 with low *Ccr9* expression, while d/d cells differentiated toward cluster 1 with high *Ccr9* expression (Figure 5B; Figure S5B). These results reveal *Ccr9* as a marker that can define strong versus less strong TCR signaling functional bifurcation.

We next characterized how gene expression changes as b/d KN6 cells differentiate into the  $\gamma\delta$  NKT cell lineage (cluster 2) and as d/d KN6 cells differentiate into the innate  $\gamma\delta$ T17 lineage (cluster 8). From cluster 6 to cluster 1 to cluster 2, b/d cells lacked *Ccr9* expression (Figure 5C). *Klrk1* (NKG2D), which functions as an NK activating receptor (Crinier et al., 2018), was initially low in expression but gradually increased and sustained upon full differentiation (Figure 5C; Figure S5C). *Klrk1* (CD94) and *Klrc1* (NKG2A), which together function as an NK inhibitory receptor (Crinier et al., 2018), had *Klrk1* being expressed early on and gradually increased and sustained upon full differentiation, while *Klrc1* was not detected until late in differentiation (Figure 5C; Figure S5C). From cluster 6 to cluster 1, d/d cells greatly increased their *Ccr9* expression, which was lowered but sustained in cluster 8 (Figure 5C). *Blk* was expressed early on, and its levels were consistent upon full differentiation, while *Maf* was initially low in expression, but its levels peaked in cluster 1 and maintained upon full differentiation, while *Rorc* expression was not detected until late in differentiation (Figure 5C; Figure S5C). Altogether, these results reveal the temporal kinetics of expression of key genes that define specific functional fates.

### $\gamma\delta$ lineage commitment in T cell progenitors is Notch independent *in vivo*

Notch is required for DN3 transition to the CD4<sup>+</sup>CD8<sup>+</sup> double-positive (DP) stage, whereas it is dispensable for DN3 commitment to the  $\gamma\delta$  lineage *in vitro* (Ciofani et al., 2006). It remained to be determined whether this is also observed *in vivo*. To address this, we Dox-treated RBPJ<sup>ind</sup> mice for 5 days to generate DN2/DN3 cells in the thymus, as previously described (Chen et al., 2019) (Figure S6A). Dox treatment was then continued or discontinued for 7 days, because both DP and  $\gamma\delta$ TCR<sup>+</sup>CD73<sup>+</sup>  $\gamma\delta$  lineage cells arose after 12 days of T cell development (Figures S6B and S6C). Mice with continued Dox treatment (Dox<sup>+5d+7d</sup>) showed robust appearance of DP,  $\gamma\delta$ TCR<sup>+</sup>CD73<sup>-</sup>, and  $\gamma\delta$ TCR<sup>+</sup>CD73<sup>+</sup> cells (Figures S7A and S7B). Mice with discontinued Dox treatment (Dox<sup>+5d-7d</sup>) showed an absence of DP cells, had reduced  $\gamma\delta$ TCR<sup>+</sup>CD73<sup>-</sup> cells, but still developed  $\gamma\delta$ TCR<sup>+</sup>CD73<sup>+</sup> cells (Figures S7A and S7B). These results suggest that Notch signaling is dispensable for  $\gamma\delta$  lineage commitment in T cell progenitors *in vivo*.

### Notch inhibits $\gamma\delta$ T1 differentiation with less strong TCR signals

Both b/d and d/d RBPJ<sup>ind</sup>KN6<sup>tg</sup> mice were Dox treated for 8 days to generate a wave of T cells; then Dox was continued (Dox<sup>+8d+4d</sup>) or discontinued (Dox<sup>+8d-4d</sup>) for 4 days. The number of thymic KN6 cells was not significantly reduced in b/d Dox<sup>+8d-4d</sup> mice compared with b/d Dox<sup>+8d+4d</sup> mice but was significantly reduced in d/d Dox<sup>+8d-4d</sup> mice compared with d/d Dox<sup>+8d+4d</sup> mice (Figure S8A). In b/d mice, whether Notch responsiveness was sustained or ceased, thymic KN6 cells showed CD73<sup>hi</sup> expression, suggesting that Notch does not affect  $\gamma\delta$  lineage commitment with strong TCR signals (Figure S8A). Conversely, in d/d mice, more thymic KN6 cells showed CD73<sup>lo</sup> expression when Notch responsiveness was ceased, suggesting that Notch inhibits  $\gamma\delta$  lineage commitment with less strong TCR signals (Figure S8A).

In b/d RBPJ<sup>ind</sup>KN6<sup>tg</sup> mice,  $\gamma\delta$ T1 cells were found within the CD73<sup>hi</sup> population, and regardless of whether Notch responsiveness was sustained or ceased, the percentage of CD73<sup>+</sup>IFN $\gamma$ <sup>+</sup> cells did not change, but the number of CD73<sup>+</sup>IFN $\gamma$ <sup>+</sup> cells was reduced when

Notch responsiveness was ceased (Figure 6A). Nevertheless, the IFN $\gamma$  MFI was similar, suggesting that Notch is not required for  $\gamma\delta$ T1 differentiation with strong TCR signals (Figure 6A). In contrast, in d/d RBPJ<sup>ind</sup>KN6<sup>tg</sup> mice,  $\gamma\delta$ T1 cells were found within the CD73<sup>-</sup> or CD73<sup>lo</sup> population, when Notch responsiveness was sustained or ceased, respectively (Figure 6A). Of note, the percentage and number of CD73<sup>+</sup>IFN $\gamma$ <sup>+</sup> cells, as well as the IFN $\gamma$  MFI, were significantly increased when Notch responsiveness was ceased (Figure 6A). These data suggest that Notch inhibits  $\gamma\delta$ T1 differentiation with less strong TCR signals.

### Notch promotes $\gamma\delta$ T2 generation

T cell development in b/d Dox<sup>+8d+4d</sup> RBPJ<sup>ind</sup>KN6<sup>tg</sup> mice generated thymic KN6 cells with IL-4-producing capacity, but there was a near absence of  $\gamma\delta$ T2 cells in d/d Dox<sup>+8d+4d</sup> RBPJ<sup>ind</sup>KN6<sup>tg</sup> mice (Figure 6B). This demonstrates that  $\gamma\delta$ T2 differentiation is also mediated by strong TCR signals in these mice. Of note, b/d Dox<sup>+8d-4d</sup> mice showed a significant decrease in the percentages and numbers of IL-4<sup>+</sup> populations compared with b/d Dox<sup>+8d+4d</sup> mice (Figure 6B). These results suggest that in combination with strong TCR signals, Notch also promotes  $\gamma\delta$ T2 (and thus  $\gamma\delta$  NKT cell) differentiation.

T cell development in d/d Dox<sup>+8d+4d</sup> RBPJ<sup>ind</sup>KN6<sup>tg</sup> mice generated thymic KN6 cells with IL-17-producing capacity, but there was a near absence of  $\gamma\delta$ T17 cells in b/d Dox<sup>+8d+4d</sup> RBPJ<sup>ind</sup>KN6<sup>tg</sup> mice (Figure S8B). This demonstrates that  $\gamma\delta$ T17 differentiation is also mediated by less strong TCR signals in these mice. Of note, d/d Dox<sup>+8d-4d</sup> mice did not show differences in their ability to generate  $\gamma\delta$ T17 cells compared with d/d Dox<sup>+8d+4d</sup> mice (Figure S8B). These results suggest that  $\gamma\delta$ T17 differentiation does not require ongoing Notch signaling *in vivo*.

### Transcriptomic analysis of Notch regulation in b/d and d/d thymic KN6 cells

To further elucidate the role of Notch signaling in  $\gamma\delta$  T cell functional programming with strong TCR signals, we performed scRNA-seq on thymic KN6 cells from b/d Dox<sup>+8d+4d</sup> (+ +) and b/d Dox<sup>+8d-4d</sup> (+ -) RBPJ<sup>ind</sup>KN6<sup>tg</sup> mice. In total, 2,775 b/d++ and 3,065 b/d+- cells were analyzed, in which UMAP analysis revealed 12 clusters (Figure 6C), with the genes enriched in each cluster listed in Table S4. Interestingly, both b/d++ and b/d+- contained cluster 8 cells that shared similar gene expressions with innate  $\gamma\delta$ T17 cells from d/d KN6<sup>tg</sup> mice. These include genes that we interpreted as early  $\gamma\delta$ T17 genes, such as *Maf*, and others, such as *Cxcr6*, *Gpr183*, and *Il18r1* (Table S4). However, b/d++ and b/d+- cluster 8 cells did not express genes that we interpreted as late  $\gamma\delta$ T17 genes, such as *Rorc*, and others, such as *Ccr6*, *Il1r1*, and *Il23r* (Table S4). This suggests that an early wave of T cell development can generate  $\gamma\delta$  T cells with IL-17 potential with strong TCR signals, but they are not fully programmed for the  $\gamma\delta$ T17 fate in the thymus. Of note, b/d+- contained more cluster 2 cells compared with b/d++ (Figure 6C). Cluster 2 had enriched expression of genes present in IELs from b/d KN6<sup>tg</sup> mice, such as *Cd7*, *Itgae*, and *Itgal* (Table S4).

We next investigated how Notch regulates  $\gamma\delta$  NKT cell differentiation. Twelve days of T cell development did not generate substantial numbers of fully differentiated  $\gamma\delta$  NKT cells (cluster 10), which had enriched expression of genes found in cluster 2 from b/d KN6<sup>tg</sup>

mice, such as *Klrk1*, *Klrk1l*, and *Klrc1* (Figure 6C; Table S4). Although cluster 10 had features of fully differentiated  $\gamma\delta$  NKT cells, the gene expression profile of cluster 1 was consistent with  $\gamma\delta$  NKT cell progenitors, and b/d++ contained significantly more cluster 1 cells compared with b/d+- (Figure 6C; Table S3). Of importance, cluster 1 had enriched expression of *Hivep3*, which is shown to be expressed in NKT cell progenitors and required for the survival, differentiation, and function of NKT cells (Harsha Krovi et al., 2020) (Figure S9A; Table S4). Other genes that defined cluster 1 and that may be involved in  $\gamma\delta$  NKT cell programming included *Tnfrsf9*, *Xcl1*, and *Nrgn* (Figure S9A; Table S4). Although *Zbtb16* (PLZF) was not enriched in any particular cluster, it was expressed in cluster 1 (Figure S9B). Analysis of *Hivep3* and *Zbtb16* within cluster 1 showed that b/d++ contained more overlapping expression of the two genes compared with b/d+-, and the ratio of *Hivep3*<sup>+</sup>*Zbtb16*<sup>+</sup> cells to other cells was significantly higher in b/d++ compared with b/d+- (Figure S9B; Table S3). Altogether, these results demonstrate the role of Notch in maintaining  $\gamma\delta$  NKT cell progenitors to enforce  $\gamma\delta$ T2 differentiation.

To further elucidate the role of Notch signaling in  $\gamma\delta$  T cell functional programming with less strong TCR signals, we performed scRNA-seq on thymic KN6 cells from d/d Dox<sup>+8d+4d</sup> (++) and d/d Dox<sup>+8d-4d</sup> (+-) RBPJ<sup>ind</sup>KN6<sup>tg</sup> mice. In total, 2,505 d/d++ and 3,568 d/d+- cells were analyzed, in which UMAP analysis revealed 12 clusters (Figure 7A), with the genes enriched in each cluster listed in Table S5. Of note, the clearest significant difference between d/d++ and d/d+- was cluster 2, which was nearly absent in the former but very evident in the latter (Figure 7A; Table S3). Among the genes enriched in cluster 2 include *Sox4*, similar to KN6<sup>tg</sup> committed  $\gamma\delta$  T cell progenitors (Table S5). Further analysis of the genes enriched in cluster 2 revealed *Ccr9*, which we described as denoting committed  $\gamma\delta$  T cell progenitors with less strong TCR signals, and *Sox13*, another previously described  $\gamma\delta$  lineage differentiation gene (Melichar et al., 2007) (Figure 7B; Table S5). These results reinforce our findings indicating that alleviation of Notch responsiveness can enhance  $\gamma\delta$  lineage commitment in d/d mice. Cluster 2 also showed upregulation of *Sh2d1a*, which encodes for signaling lymphocytic activation molecule (SLAM)-associated protein (SAP) and is important for acquisition of IFN $\gamma$  production (Dienz et al., 2020), and upregulation of *Gzma* (Figure 7B; Table S5). These results reinforce our findings indicating that alleviation of Notch responsiveness can enhance IFN $\gamma$  production in d/d mice, and reveal that cytotoxic properties are also inhibited by Notch with less strong TCR signals.

In addition to d/d+- containing more cluster 2 cells, on a per-cell basis, d/d+- cluster 2 cells expressed higher levels of *Ccr9* and *Sh2d1a* compared with the few d/d++ cluster 2 cells (Figure 7C). Moreover, d/d+- cluster 2 cells showed higher levels of *Id3*, which is typically upregulated by strong TCR signals to inhibit E-protein activity and promote  $\gamma\delta$ -lineage commitment (Lauritsen et al., 2009), and higher levels of *Hspa1b*, a member of the heat shock protein 70 family that is implicated in T cell cytotoxicity (Figueiredo et al., 2009) (Figure 7C). Both d/d++ and d/d+- contained cluster 1 cells; however, their UMAP positions are distinctly different (Figure 7D). On a per-cell basis, d/d+- cluster 1 cells displayed higher levels of *Dapl1* compared with d/d++ cluster 1 cells, which likely defines mature naive  $\gamma\delta$  T cells (Figure 7D). Altogether, these results illustrate the role of Notch in regulating  $\gamma\delta$  lineage commitment and functional differentiation with less strong TCR signals.

## DISCUSSION

In this study, we used RBPJ<sup>ind</sup>, KN6<sup>tg</sup>, and RBPJ<sup>ind</sup>KN6<sup>tg</sup> mice to address the roles of ontogenic timing, TCR signal strength, and Notch signaling in  $\gamma\delta$  T cell functional differentiation *in vivo*. Temporal restriction of T cell development revealed that the fetal period allowed for a biased generation of V $\gamma$ 1<sup>+</sup> cells toward the PLZF<sup>+</sup>Lin28b<sup>+</sup> lineage and a favored, but not exclusive, generation of  $\gamma\delta$ T17 cells. Lung  $\gamma\delta$ T17 functionality in response to TDM was shown to be Notch independent. Modulation of TCR and Notch signaling in developing  $\gamma\delta$  T cells revealed that IL-4 differentiation required strong TCR signals and Notch, while IL-17 differentiation required less strong TCR signals but was Notch independent.

Generation of V $\gamma$ 1<sup>+</sup> cells was limited during the fetal period, but fetal V $\gamma$ 1<sup>+</sup> cells were enriched for PLZF and Lin28b expression. Having Lin28b may reflect the need for fetal V $\gamma$ 1<sup>+</sup> cells to proliferate as mature cells, because the fetal thymus generates fewer V $\gamma$ 1<sup>+</sup> cells compared with the adult thymus. Lin28b would also allow fetal V $\gamma$ 1<sup>+</sup> cells to persist long term through self-renewal. Although fetal  $\gamma\delta$ T17 cells are innate-like, post-natal  $\gamma\delta$ T17 cells are likely adaptive and thus not pre-programmed for the IL-17 fate. However, they maintain an IL-17-permissive chromatin state (Schmolka et al., 2013) and require peripheral activation to produce IL-17 (Chien et al., 2013; Jouan et al., 2018). An example of adaptive  $\gamma\delta$ T17 cells is phycoerythrin-specific  $\gamma\delta$  T cells (Zeng et al., 2012). Thus, ontogenic timing may be a driving factor in innate-like versus adaptive  $\gamma\delta$  T cell differentiation.

ID3 deficiency increases the number of  $\gamma\delta$  NKT cells (Alonzo et al., 2010; Lauritsen et al., 2009). However, it was unclear whether  $\gamma\delta$ T2 development requires strong TCR signals but becomes susceptible to cell death. If so, ID3 deficiency may attenuate TCR signals to a degree that permits  $\gamma\delta$ T2 differentiation but allows for survival. Alternatively,  $\gamma\delta$ T2 development may be inhibited by strong TCR signals (Miyazaki et al., 2015; Zhang et al., 2018). Using KN6<sup>tg</sup> mice, we demonstrated that  $\gamma\delta$ T2 cells develop only with strong TCR signals. IL-17 functionality was enhanced with less strong TCR signals. This observation is consistent with *in vitro* findings (Zarin et al., 2018). However, we additionally showed that innate-like  $\gamma\delta$ T17 generation occurs only with less strong TCR signals. Interestingly, IFN $\gamma$ <sup>+</sup>IL-17<sup>+</sup> thymic KN6 cells were increased with strong TCR signals. These  $\gamma\delta$  T cells can arise from pro-inflammatory tumor environments (Schmolka et al., 2013). It has been disputed whether  $\gamma\delta$ T17 cells develop with weak or absent ligand engagement (Coffey et al., 2014; Haks et al., 2005; Jensen et al., 2008; Spidale et al., 2018). We showed that IL-17<sup>+</sup> thymic KN6 cells were CD73<sup>+</sup>, suggesting that they were not antigen naive. Our scRNA-seq analysis provided insights into the genetic programs that regulate strong versus less strong TCR signaling divergence, which included differential *Ccr9* expression. This approach also defined early, intermediate, and late genes involved in  $\gamma\delta$  NKT cell or innate  $\gamma\delta$ T17 differentiation.

We showed in RBPJ<sup>ind</sup> mice that  $\gamma\delta$  lineage commitment in T cell progenitors is Notch independent, validating *in vitro* findings (Ciofani et al., 2006). It has also been suggested that Notch signaling negatively regulates  $\gamma\delta$  T cell differentiation (Tanigaki et al., 2004;

Washburn et al., 1997). Using RBPJ<sup>ind</sup>KN6<sup>tg</sup> mice, we demonstrated that Notch could inhibit  $\gamma\delta$  T cell differentiation with less strong TCR signals, but not with strong TCR signals. Our transcriptomic analysis revealed that this was due to enhanced generation of a *Ccr9*-expressing population that is poised for IFN $\gamma$  and cytotoxicity when Notch responsiveness was removed. This analysis also revealed that Notch maintains *Hivep3*-expressing  $\gamma\delta$  NKT cell progenitors for  $\gamma\delta$ T2 cells.

### Limitations of the study

We noted that some key observations in our study appear to contradict previous findings. We showed that Notch signaling in fetal-derived lung  $\gamma\delta$  T cells does not influence IL-17 production in response to TDM. This is in contrast with a report showing a reduction in IL-17 production by *Hes1* deletion (Shibata et al., 2011). This suggests that *Hes1* expression in peripheral  $\gamma\delta$  T cells may be regulated independently of RBPJ-dependent Notch signaling (Nakamura et al., 2015). We did not observe Notch exerting an effect on  $\gamma\delta$ T17 development, contrary to *in vitro* findings (Zarin et al., 2018). This suggests that the thymus microenvironment may provide additional factors that can compensate for Notch function *in vivo*.

In this study we took advantage of RBPJ<sup>ind</sup>, KN6<sup>tg</sup>, and RBPJ<sup>ind</sup>KN6<sup>tg</sup> mouse models. By analyzing only fetal, neonatal, or adult  $\gamma\delta$  T cells exclusively, we may not fully consider the complexity of interactions that occur between  $\gamma\delta$  T cells arising from different time periods in RBPJ<sup>ind</sup> mice. An obvious limitation with KN6<sup>tg</sup> mice is that they do not account for clonal variations and other antigen specificities that may influence  $\gamma\delta$  T cell programming. Nevertheless, taken together, the experimental approach allowed us to precisely define the roles of ontogenic timing, TCR signal strength, and Notch signaling in  $\gamma\delta$  T cell functional differentiation *in vivo*.

## STAR★METHODS

### RESOURCE AVAILABILITY

**Lead contact**—Further information and requests for resources and reagents should be directed to and will be fulfilled by the lead contact, Juan Carlos Zúñiga-Pflücker (jczp@sri.utoronto.ca).

**Materials availability**—All resources and reagents used in this study are available upon request from the lead contact.

**Data and code availability**—The data that support the findings of this study are available upon request from the lead contact. Raw and processed RNA-seq and scRNA-seq data are available from the Gene Expression Omnibus (GEO). The accession number for the RNA-seq data reported in this paper is GEO: GSE166086. The accession number for the scRNA-seq data reported in this paper is GEO: GSE165908.

## EXPERIMENTAL MODEL AND SUBJECT DETAILS

**Mice**—All mice were bred and maintained in the Comparative Research facility at Sunnybrook Research Institute under specific pathogen-free conditions. All animal procedures were approved by the Sunnybrook Research Institute Animal Care Committee and performed in accordance with the committee's ethical standards. For studies involving the RBPJ<sup>ind</sup> mouse model, mice were Dox-treated from conception to birth, from birth to 3 weeks of age, or from 6–9 weeks of age for fetal, neonatal, or adult specific induction of T cell development, respectively. Mice were then analyzed at 12 weeks of age. For studies involving the KN6<sup>tg</sup> mouse model, mice were analyzed at 10 weeks of age. For studies involving the RBPJ<sup>ind</sup>KN6<sup>tg</sup> mouse model, 8 week old mice were Dox-treated for 8 days, and then the Dox treatment was continued or discontinued for 4 days, upon which mice were then analyzed. Male and female mice were used in all experiments but were sex-matched for each condition.

## METHOD DETAILS

**Induction of notch responsiveness**—To induce RBPJ-HA expression *in vivo*, RBPJ<sup>ind</sup> and RBPJ<sup>ind</sup>KN6<sup>tg</sup> mice were injected with 2 mg/ml Dox (Sigma-Aldrich) intraperitoneally at time “0,” and administered 1 mg/ml Dox in drinking water supplemented with 5% Splenda *ad libitum* for the duration of the experiment, with drinking water changed twice every week. Mice not receiving Dox were given drinking water supplemented with 5% Splenda alone.

**Cell preparation**—Single-cell suspensions were prepared from mouse thymus, spleen, lymph node, lung, epidermis, and intestinal epithelium. Lungs were first digested with 2 mg/ml collagenase A (Roche) in 37°C shaker for 1 hour. Ear skin was first incubated with 20 mM EDTA in 37°C for 1 hour to allow separation of epidermis from dermis. Small intestines were first incubated with 5 mM EDTA and 0.15 mg/ml DTT (Sigma-Aldrich) in 37°C shaker for 30 minutes to allow separation of intestinal epithelium from lamina propria. All tissues were passed through cell strainers while in  $\alpha$ -Minimum Essential Medium Eagle containing 15% fetal bovine serum and 1% penicillin-streptomycin ( $\alpha$ -MEM) to obtain single-cell suspensions. Erythrocytes were lysed using BD Pharm Lyse (BD Biosciences).

***In vitro* stimulation**—Cells were incubated in 37°C for 5 hours while in  $\alpha$ -MEM. Unstimulated samples were cultured with brefeldin A (eBiosciences) alone. Stimulated samples were cultured with brefeldin A, and with 100 ng/ml PMA (Sigma-Aldrich) and 1  $\mu$ g/ml ionomycin (Sigma-Aldrich) to detect IFN $\gamma$ , IL-4, and IL-17 production, or with 10 ng/ml IL-1 $\beta$  (R&D Systems) and 10 ng/ml IL-23 (R&D Systems) to detect IL-17 production.

**TDM inflammation model**—150  $\mu$ g TDM (Sigma-Aldrich) was prepared as an oil-in-water emulsion containing 9% mineral oil (Sigma-Aldrich), 1% Tween-80 (Sigma-Aldrich), and 90% saline. Emulsion without TDM served as mock controls. TDM and mock emulsions were intravenously injected into mice, and lung  $\gamma\delta$  T cell IL-17 production was analyzed *ex vivo* 2 days later without further stimulation.

**Flow cytometry**—Single-cell suspensions were stained with antibodies against cell-surface antigens while in Hanks' Balanced Salt Solution containing 1% bovine serum albumin and 2 mM EDTA. To detect intracellular cytokines and transcription factors, cells were then fixed, permeabilized, and intracellularly stained using BD Fixation/Permeabilization Solution Kit (BD Biosciences). Antibodies were purchased from BD Biosciences, eBiosciences, or BioLegend. Flow cytometry was performed using BD LSR II and data analyzed using FlowJo version 9.9.6.

**RNA sequencing**—Mature CD24<sup>-</sup> V $\gamma$ 1<sup>+</sup> cells (pre-gated on CD3<sup>+</sup>  $\gamma$   $\delta$  TCR<sup>+</sup>) were sorted from thymi using BD FACSAria Fusion. RNA was extracted using TRIzol. Library construction was done using Takara SMARTer Stranded Total RNA-Seq Kit v3 – Pico Input Mammalian. RNA-seq was performed using Illumina NovaSeq 6000. Raw data were aligned to GRCm38 using HISAT2 version 2.1 and raw read counts were obtained using HTSeq version 0.1. Raw read counts were normalized, and differential gene expression analysis was performed using R software version 3.6.3 with the package edgeR version 1.

**Single-cell RNA sequencing**—CD3<sup>+</sup> V $\gamma$ 4<sup>+</sup> KN6 cells were sorted from thymi using BD FACSAria Fusion. Library construction was done using 10x Genomics Chromium Controller v3. Single-cell RNA-seq was performed using Illumina NovaSeq 6000. Raw data were aligned to GRCm38, and raw read counts were obtained using Cell Ranger version 5.0. Raw read counts were normalized, samples were integrated (eliminating batch differences), cells were clustered, and differential gene expression analysis was performed using R software version 3.6.3 with the package Seurat version 3. Pseudotime analysis and construction of cell trajectories was performed using R software version 3.6.3 with the package Monocle version 3.

## QUANTIFICATION AND STATISTICAL ANALYSIS

The data and error bars are presented as mean  $\pm$  standard deviation. To determine statistical significance, a two-tailed unpaired t test (comparing two means) or a one-way ANOVA (comparing three or more means) was performed using Prism version 6. Statistical significance was determined as ns = not significant, \* $p < 0.05$ , \*\* $p < 0.01$ , \*\*\* $p < 0.001$ , \*\*\*\* $p < 0.0001$ . For RNA-seq analysis, significantly upregulated genes were determined using empirical Bayes moderated t-statistics, where significance was determined as  $p < 0.05$ . For scRNA-seq analysis, significantly upregulated genes were determined using a Wilcoxon rank sum test, and significantly changed cell cluster distributions were determined using a chi-square test, where significance was determined as  $p < 0.05$ . Statistical details (including the value of  $n$  and what  $n$  represents) are found in figure, supplemental figure, and supplemental table legends.

## Supplementary Material

Refer to Web version on PubMed Central for supplementary material.

## ACKNOWLEDGMENTS

We are grateful to Lisa Wells for assistance with animal care and to Geneve Awong and Paul Oleynik for assistance with cell sorting. The graphical abstract was created using BioRender. This work was supported by grants from the Canadian Institutes of Health Research (CIHR FND-154332), National Institutes of Health (NIH-1P01AI102853-01), and the Krembil Foundation. E.L.Y.C. was supported by an Ontario Graduate Scholarship. P.K.T. was supported by a Banting and Best Doctoral Research Award. J.C.Z.-P. is supported by a Canada Research Chair in Developmental Immunology.

## REFERENCES

- Adams EJ, Strop P, Shin S, Chien YH, and Garcia KC (2008). An autonomous CDR3delta is sufficient for recognition of the nonclassical MHC class I molecules T10 and T22 by gammadelta T cells. *Nat. Immunol* 9, 777–784. [PubMed: 18516039]
- Akitsu A, and Iwakura Y (2018). Interleukin-17-producing  $\gamma\delta$  T ( $\gamma\delta$ 17) cells in inflammatory diseases. *Immunology* 155, 418–426. [PubMed: 30133701]
- Alonzo ES, Gottschalk RA, Das J, Egawa T, Hobbs RM, Pandolfi PP, Pereira P, Nichols KE, Koretzky GA, Jordan MS, and Sant'Angelo DB (2010). Development of promyelocytic zinc finger and ThPOK-expressing innate gamma delta T cells is controlled by strength of TCR signaling and Id3. *J. Immunol* 184, 1268–1279. [PubMed: 20038637]
- Aono A, Enomoto H, Yoshida N, Yoshizaki K, Kishimoto T, and Komori T (2000). Forced expression of terminal deoxynucleotidyl transferase in fetal thymus resulted in a decrease in gammadelta T cells and random dissemination of Vgamma3Vdelta1 T cells in skin of newborn but not adult mice. *Immunology* 99, 489–497. [PubMed: 10792495]
- Bendelac A, Savage PB, and Teyton L (2007). The biology of NKT cells. *Annu. Rev. Immunol* 25, 297–336. [PubMed: 17150027]
- Cai Y, Xue F, Fleming C, Yang J, Ding C, Ma Y, Liu M, Zhang HG, Zheng J, Xiong N, and Yan J (2014). Differential developmental requirement and peripheral regulation for dermal V $\gamma$ 4 and V $\gamma$ 6T17 cells in health and inflammation. *Nat. Commun* 5, 3986. [PubMed: 24909159]
- Cao J, Spielmann M, Qiu X, Huang X, Ibrahim DM, Hill AJ, Zhang F, Mundlos S, Christiansen L, Steemers FJ, et al. (2019). The single-cell transcriptional landscape of mammalian organogenesis. *Nature* 566, 496–502. [PubMed: 30787437]
- Carding SR, and Egan PJ (2002). Gammadelta T cells: functional plasticity and heterogeneity. *Nat. Rev. Immunol* 2, 336–345. [PubMed: 12033739]
- Chen ELY, Thompson PK, and Zúñiga-Pflücker JC (2019). RBPJ-dependent Notch signaling initiates the T cell program in a subset of thymus-seeding progenitors. *Nat. Immunol* 20, 1456–1468. [PubMed: 31636466]
- Chien YH, Zeng X, and Prinz I (2013). The natural and the inducible: interleukin (IL)-17-producing  $\gamma\delta$  T cells. *Trends Immunol* 34, 151–154. [PubMed: 23266231]
- Ciofani M, Knowles GC, Wiest DL, von Boehmer H, and Zúñiga-Pflücker JC (2006). Stage-specific and differential notch dependency at the alphabeta and gammadelta T lineage bifurcation. *Immunity* 25, 105–116. [PubMed: 16814577]
- Coffey F, Lee SY, Buus TB, Lauritsen JP, Wong GW, Joachims ML, Thompson LF, Zúñiga-Pflücker JC, Kappes DJ, and Wiest DL (2014). The TCR ligand-inducible expression of CD73 marks  $\gamma\delta$  lineage commitment and a metastable intermediate in effector specification. *J. Exp. Med* 211, 329–343. [PubMed: 24493796]
- Crinier A, Milpied P, Escalière B, Piperoglou C, Galluso J, Balsamo A, Spinelli L, Cervera-Marzal I, Ebbo M, Girard-Madoux M, et al. (2018). High-Dimensional Single-Cell Analysis Identifies Organ-Specific Signatures and Conserved NK Cell Subsets in Humans and Mice. *Immunity* 49, 971–986.e5. [PubMed: 30413361]
- Dienz O, DeVault VL, Musial SC, Mistri SK, Mei L, Baraev A, Dragon JA, Kremontsov D, Veillette A, and Boyson JE (2020). Critical Role for SLAM/SAP Signaling in the Thymic Developmental Programming of IL-17- and IFN- $\gamma$ -Producing  $\gamma\delta$  T Cells. *J. Immunol* 204, 1521–1534. [PubMed: 32024701]

- Fahl SP, Coffey F, Kain L, Zarin P, Dunbrack RL Jr., Teyton L, Zúñiga-Pflücker JC, Kappes DJ, and Wiest DL (2018). Role of a selecting ligand in shaping the murine  $\gamma\delta$ -TCR repertoire. *Proc. Natl. Acad. Sci. USA* 115, 1889–1894. [PubMed: 29432160]
- Figueiredo C, Wittmann M, Wang D, Dressel R, Seltsam A, Blasczyk R, and Eiz-Vesper B (2009). Heat shock protein 70 (HSP70) induces cytotoxicity of T-helper cells. *Blood* 113, 3008–3016. [PubMed: 19018093]
- Gray EE, Ramírez-Valle F, Xu Y, Wu S, Wu Z, Karjalainen KE, and Cyster JG (2013). Deficiency in IL-17-committed V $\gamma$ 4(+)  $\gamma\delta$  T cells in a spontaneous Sox13-mutant CD45.1(+) congenic mouse substrain provides protection from dermatitis. *Nat. Immunol* 14, 584–592. [PubMed: 23624556]
- Haas JD, Ravens S, Düber S, Sandrock I, Oberdörfer L, Kashani E, Chennupati V, Föhse L, Naumann R, Weiss S, et al. (2012). Development of interleukin-17-producing  $\gamma\delta$  T cells is restricted to a functional embryonic wave. *Immunity* 37, 48–59. [PubMed: 22770884]
- Haks MC, Lefebvre JM, Lauritsen JP, Carleton M, Rhodes M, Miyazaki T, Kappes DJ, and Wiest DL (2005). Attenuation of gammadeltaTCR signaling efficiently diverts thymocytes to the alpha beta lineage. *Immunity* 22, 595–606. [PubMed: 15894277]
- Harsha Krovi S, Zhang J, Michaels-Foster MJ, Brunetti T, Loh L, Scott-Browne J, and Gapin L (2020). Thymic iNKT single cell analyses unmask the common developmental program of mouse innate T cells. *Nat. Commun* 11, 6238. [PubMed: 33288744]
- Havran WL, and Allison JP (1990). Origin of Thy-1+ dendritic epidermal cells of adult mice from fetal thymic precursors. *Nature* 344, 68–70. [PubMed: 1968230]
- Heilig JS, and Tonegawa S (1986). Diversity of murine gamma genes and expression in fetal and adult T lymphocytes. *Nature* 322, 836–840. [PubMed: 2943999]
- Hwang SS, Lim J, Yu Z, Kong P, Sefik E, Xu H, Harman CCD, Kim LK, Lee GR, Li HB, and Flavell RA (2020). mRNA destabilization by BTG1 and BTG2 maintains T cell quiescence. *Science* 367, 1255–1260. [PubMed: 32165587]
- Ikuta K, Kina T, MacNeil I, Uchida N, Peault B, Chien YH, and Weissman IL (1990). A developmental switch in thymic lymphocyte maturation potential occurs at the level of hematopoietic stem cells. *Cell* 62, 863–874. [PubMed: 1975515]
- In TSH, Trotman-Grant A, Fahl S, Chen ELY, Zarin P, Moore AJ, Wiest DL, Zúñiga-Pflücker JC, and Anderson MK (2017). HEB is required for the specification of fetal IL-17-producing  $\gamma\delta$  T cells. *Nat. Commun* 8, 2004. [PubMed: 29222418]
- Ito K, Van Kaer L, Bonneville M, Hsu S, Murphy DB, and Tonegawa S (1990). Recognition of the product of a novel MHC TL region gene (27b) by a mouse gamma delta T cell receptor. *Cell* 62, 549–561. [PubMed: 2379238]
- Jensen KD, Su X, Shin S, Li L, Youssef S, Yamasaki S, Steinman L, Saito T, Locksley RM, Davis MM, et al. (2008). Thymic selection determines gammadelta T cell effector fate: antigen-naive cells make interleukin-17 and antigen-experienced cells make interferon gamma. *Immunity* 29, 90–100. [PubMed: 18585064]
- Jouan Y, Patin EC, Hassane M, Si-Tahar M, Baranek T, and Paget C (2018). Thymic Program Directing the Functional Development of  $\gamma\delta$ T17 Cells. *Front. Immunol* 9, 981. [PubMed: 29867959]
- Kashani E, Föhse L, Raha S, Sandrock I, Oberdörfer L, Koenecke C, Suerbaum S, Weiss S, and Prinz I (2015). A clonotypic V $\gamma$ 4J $\gamma$ 1/V $\delta$ 5D $\delta$ 2J $\delta$ 1 innate  $\gamma\delta$  T-cell population restricted to the CCR6<sup>+</sup>CD27<sup>-</sup> subset. *Nat. Commun* 6, 6477. [PubMed: 25765849]
- Kreslavsky T, Savage AK, Hobbs R, Gounari F, Bronson R, Pereira P, Pandolfi PP, Bendelac A, and von Boehmer H (2009). TCR-inducible PLZF transcription factor required for innate phenotype of a subset of gammadelta T cells with restricted TCR diversity. *Proc. Natl. Acad. Sci. USA* 106, 12453–12458. [PubMed: 19617548]
- Laird RM, Laky K, and Hayes SM (2010). Unexpected role for the B cell-specific Src family kinase B lymphoid kinase in the development of IL-17-producing  $\gamma\delta$  T cells. *J. Immunol.* 185, 6518–6527. [PubMed: 20974990]
- Lauritsen JP, Wong GW, Lee SY, Lefebvre JM, Ciofani M, Rhodes M, Kappes DJ, Zúñiga-Pflücker JC, and Wiest DL (2009). Marked induction of the helix-loop-helix protein Id3 promotes the

- gammadelta T cell fate and renders their functional maturation Notch independent. *Immunity* 31, 565–575. [PubMed: 19833086]
- Melichar HJ, Narayan K, Der SD, Hiraoka Y, Gardiol N, Jeannot G, Held W, Chambers CA, and Kang J (2007). Regulation of gammadelta versus alphabeta T lymphocyte differentiation by the transcription factor SOX13. *Science* 315, 230–233. [PubMed: 17218525]
- Miyazaki M, Miyazaki K, Chen S, Chandra V, Wagatsuma K, Agata Y, Rodewald HR, Saito R, Chang AN, Varki N, et al. (2015). The E-Id protein axis modulates the activities of the PI3K-AKT-mTORC1-Hif1a and c-myc/p19Arf pathways to suppress innate variant TFH cell development, thymocyte expansion, and lymphomagenesis. *Genes Dev.* 29, 409–425. [PubMed: 25691468]
- Nakamura M, Shibata K, Hatano S, Sato T, Ohkawa Y, Yamada H, Ikuta K, and Yoshikai Y (2015). A genome-wide analysis identifies a notch-RBP-J $\kappa$ -IL-7R $\alpha$  axis that controls IL-17-producing  $\gamma\delta$  T cell homeostasis in mice. *J. Immunol* 194, 243–251. [PubMed: 25429074]
- Nitta T, Muro R, Shimizu Y, Nitta S, Oda H, Ohte Y, Goto M, Yanobu-Takanashi R, Narita T, Takayanagi H, et al. (2015). The thymic cortical epithelium determines the TCR repertoire of IL-17-producing  $\gamma\delta$ T cells. *EMBO Rep.* 16, 638–653. [PubMed: 25770130]
- Papotto PH, Gonçalves-Sousa N, Schmolka N, Iseppon A, Mensurado S, Stockinger B, Ribot JC, and Silva-Santos B (2017a). IL-23 drives differentiation of peripheral  $\gamma\delta$ 17 T cells from adult bone marrow-derived precursors. *EMBO Rep.* 18, 1957–1967. [PubMed: 28855306]
- Papotto PH, Ribot JC, and Silva-Santos B (2017b). IL-17<sup>+</sup>  $\gamma\delta$  T cells as kick-starters of inflammation. *Nat. Immunol* 18, 604–611. [PubMed: 28518154]
- Parker ME, and Ciofani M (2020). Regulation of  $\gamma\delta$  T Cell Effector Diversification in the Thymus. *Front. Immunol* 11, 42. [PubMed: 32038664]
- Prinz I, Silva-Santos B, and Pennington DJ (2013). Functional development of  $\gamma\delta$  T cells. *Eur. J. Immunol* 43, 1988–1994. [PubMed: 23928962]
- Ribeiro ST, Ribot JC, and Silva-Santos B (2015). Five Layers of Receptor Signaling in  $\gamma\delta$  T-Cell Differentiation and Activation. *Front. Immunol* 6, 15. [PubMed: 25674089]
- Ribot JC, deBarros A, Pang DJ, Neves JF, Peperzak V, Roberts SJ, Girardi M, Borst J, Hayday AC, Pennington DJ, and Silva-Santos B (2009). CD27 is a thymic determinant of the balance between interferon-gamma- and interleukin 17-producing gammadelta T cell subsets. *Nat. Immunol* 10, 427–436. [PubMed: 19270712]
- Saitoh T, Yano I, Kumazawa Y, and Takimoto H (2012). Pulmonary TCR  $\gamma\delta$  T cells induce the early inflammation of granuloma formation by a glycolipid trehalose 6,6'-dimycolate (TDM) isolated from *Mycobacterium tuberculosis*. *Immunopharmacol. Immunotoxicol* 34, 815–823. [PubMed: 22963130]
- Schenkel AR, Kingry LC, and Slayden RA (2013). The *ly49* gene family. A brief guide to the nomenclature, genetics, and role in intracellular infection. *Front. Immunol* 4, 90. [PubMed: 23596445]
- Schmolka N, Serre K, Grosso AR, Rei M, Pennington DJ, Gomes AQ, and Silva-Santos B (2013). Epigenetic and transcriptional signatures of stable versus plastic differentiation of proinflammatory  $\gamma\delta$  T cell subsets. *Nat. Immunol* 14, 1093–1100. [PubMed: 23995235]
- Schmolka N, Wencker M, Hayday AC, and Silva-Santos B (2015). Epigenetic and transcriptional regulation of  $\gamma\delta$  T cell differentiation: programming cells for responses in time and space. *Semin. Immunol* 27, 19–25. [PubMed: 25726512]
- Sheridan BS, and Lefrançois L (2010). Intraepithelial lymphocytes: to serve and protect. *Curr. Gastroenterol. Rep* 12, 513–521. [PubMed: 20890736]
- Shibata K, Yamada H, Sato T, Dejima T, Nakamura M, Ikawa T, Hara H, Yamasaki S, Kageyama R, Iwakura Y, et al. (2011). Notch-Hes1 pathway is required for the development of IL-17-producing  $\gamma\delta$  T cells. *Blood* 118, 586–593. [PubMed: 21606479]
- Spidale NA, Sylvania K, Narayan K, Miu B, Frascoli M, Melichar HJ, Zhihao W, Kisielow J, Palin A, Serwold T, et al. (2018). Interleukin-17-Producing  $\gamma\delta$  T Cells Originate from SOX13<sup>+</sup> Progenitors that Are Independent of  $\gamma\delta$ TCR Signaling. *Immunity* 49, 857–872.e5. [PubMed: 30413363]
- Tanigaki K, Tsuji M, Yamamoto N, Han H, Tsukada J, Inoue H, Kubo M, and Honjo T (2004). Regulation of alphabeta/gammadelta T cell lineage commitment and peripheral T cell responses by Notch/RBP-J signaling. *Immunity* 20, 611–622. [PubMed: 15142529]

- Vantourout P, and Hayday A (2013). Six-of-the-best: unique contributions of  $\gamma\delta$  T cells to immunology. *Nat. Rev. Immunol* 13, 88–100. [PubMed: 23348415]
- Wakim LM, Gupta N, Mintern JD, and Villadangos JA (2013). Enhanced survival of lung tissue-resident memory CD8<sup>+</sup> T cells during infection with influenza virus due to selective expression of IFITM3. *Nat. Immunol* 14, 238–245. [PubMed: 23354485]
- Washburn T, Schweighoffer E, Gridley T, Chang D, Fowlkes BJ, Cado D, and Robey E (1997). Notch activity influences the alphabeta versus gammadelta T cell lineage decision. *Cell* 88, 833–843. [PubMed: 9118226]
- Weng AP, Millholland JM, Yashiro-Ohtani Y, Arcangeli ML, Lau A, Wai C, Del Bianco C, Rodriguez CG, Sai H, Tobias J, et al. (2006). c-Myc is an important direct target of Notch1 in T-cell acute lymphoblastic leukemia/lymphoma. *Genes Dev.* 20, 2096–2109. [PubMed: 16847353]
- Wong GW, and Zúñiga-Pflücker JC (2010). gammadelta and alphabeta T cell lineage choice: resolution by a stronger sense of being. *Semin. Immunol* 22, 228–236. [PubMed: 20466561]
- Xu X, Deobagkar-Lele M, Bull KR, Crockford TL, Mead AJ, Cribbs AP, Sims D, Anzilotti C, and Cornall RJ (2020). An ontogenetic switch drives the positive and negative selection of B cells. *Proc. Natl. Acad. Sci. USA* 117, 3718–3727. [PubMed: 32019891]
- Yuan J, Nguyen CK, Liu X, Kanellopoulou C, and Muljo SA (2012). Lin28b reprograms adult bone marrow hematopoietic progenitors to mediate fetal-like lymphopoiesis. *Science* 335, 1195–1200. [PubMed: 22345399]
- Zarin P, Chen EL, In TS, Anderson MK, and Zúñiga-Pflücker JC (2015). Gamma delta T-cell differentiation and effector function programming, TCR signal strength, when and how much? *Cell. Immunol* 296, 70–75. [PubMed: 25866401]
- Zarin P, In TS, Chen EL, Singh J, Wong GW, Mohtashami M, Wiest DL, Anderson MK, and Zúñiga-Pflücker JC (2018). Integration of T-cell receptor, Notch and cytokine signals programs mouse  $\gamma\delta$  T-cell effector differentiation. *Immunol. Cell Biol* 96, 994–1007. [PubMed: 29754419]
- Zeng X, Wei YL, Huang J, Newell EW, Yu H, Kidd BA, Kuhns MS, Waters RW, Davis MM, Weaver CT, and Chien YH (2012).  $\gamma\delta$  T cells recognize a microbial encoded B cell antigen to initiate a rapid antigen-specific interleukin-17 response. *Immunity* 37, 524–534. [PubMed: 22960222]
- Zhang B, Jiao A, Dai M, Wiest DL, and Zhuang Y (2018). Id3 Restricts  $\gamma\delta$  NKT Cell Expansion by Controlling Egr2 and c-Myc Activity. *J. Immunol* 201, 1452–1459. [PubMed: 30012846]
- Zuberbuehler MK, Parker ME, Wheaton JD, Espinosa JR, Salzler HR, Park E, and Ciofani M (2019). The transcription factor c-Maf is essential for the commitment of IL-17-producing  $\gamma\delta$  T cells. *Nat. Immunol* 20, 73–85. [PubMed: 30538336]

### Highlights

- Waves of  $\gamma\delta$  T cell development can be temporally regulated in RBPJ-inducible mice
- Strong TCR signals collaborate with Notch to promote  $\gamma\delta$  T cell IL-4 programming
- Less strong TCR signals promote Notch-independent IL-17 programming in  $\gamma\delta$  T cells
- *Ccr9* defines TCR signal strength-dependent bifurcation of  $\gamma\delta$  T cell functional subsets

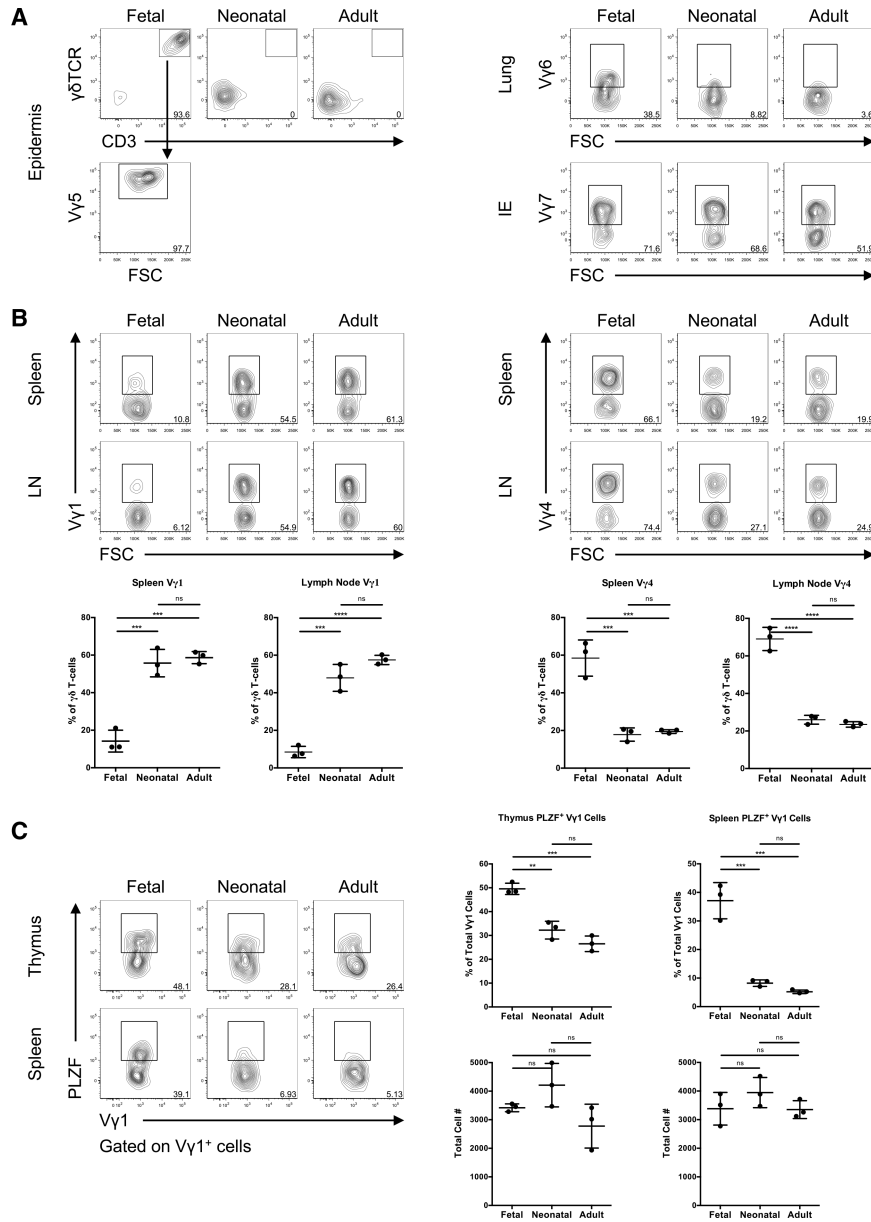


**Figure 1. Ontogenic timing influences Vγ subset generation**  
 (A) Flow cytometry analysis of Vγ5<sup>+</sup>, Vγ6<sup>+</sup>, and Vγ7<sup>+</sup> cells in epidermis, lung, and intestinal epithelium, respectively, of fetal-, neonatal-, or adult-induced RBPJ<sup>ind</sup> mice; pre-gated on γδ T cells.  
 (B) Flow cytometry analysis of Vγ1<sup>+</sup> and Vγ4<sup>+</sup> cells in spleen and lymph nodes of mice as in (A); pre-gated on γδ T cells (top); bottom panels show percentages.  
 (C) Flow cytometry analysis of PLZF<sup>+</sup> Vγ1<sup>+</sup> cells in thymus and spleen of mice as in (A) (left); right panels show percentages and numbers. Data are representative of three independent experiments.  
 Data are presented as means ± standard deviation of three independent experiments. n = 3 mice per group. \*\*p < 0.01, \*\*\*p < 0.001, \*\*\*\*p < 0.0001 (one-way ANOVA). ns, not significant.

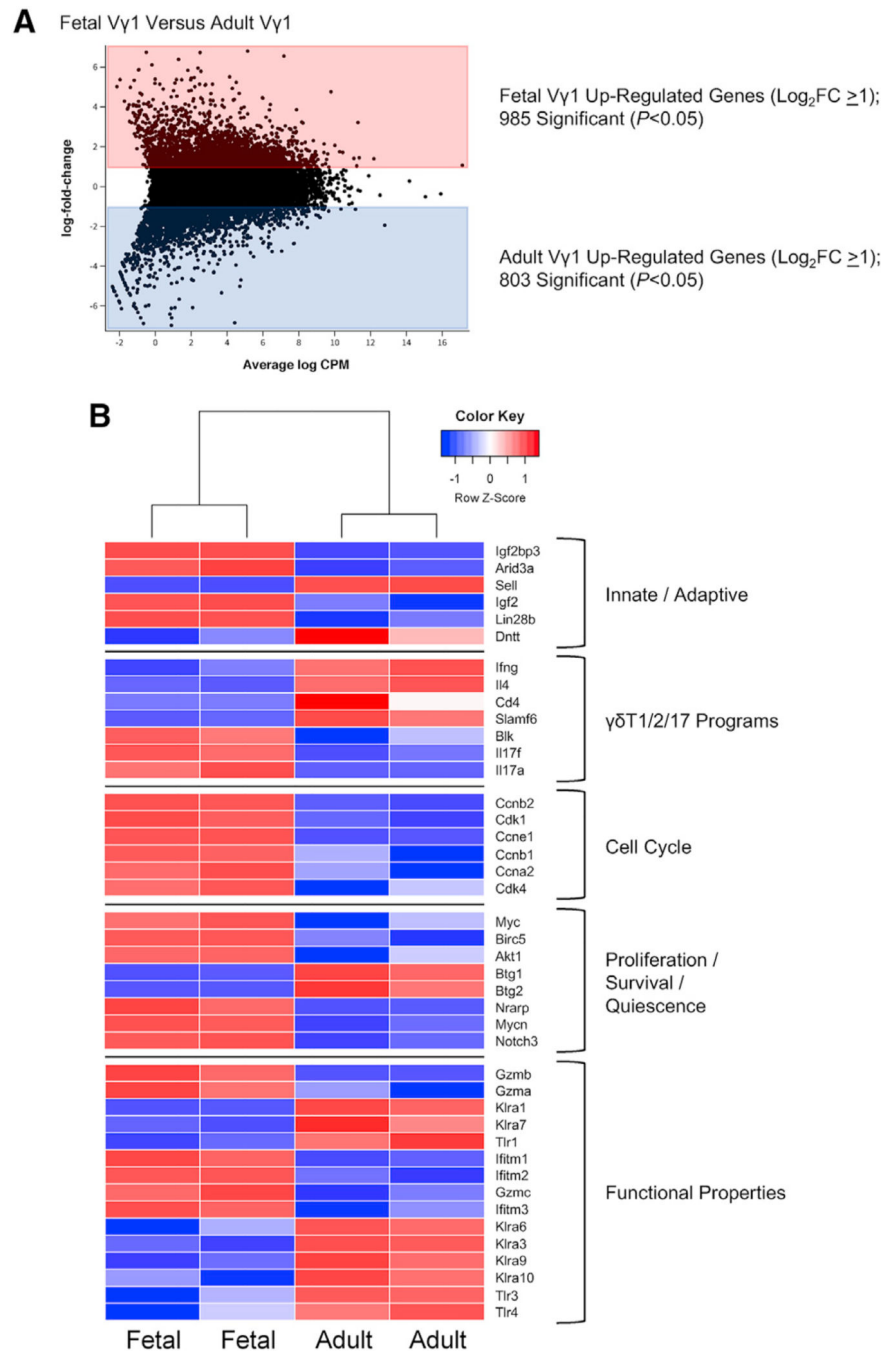


**Figure 2. Transcriptomic analysis of fetal versus adult V $\gamma$ 1<sup>+</sup> cells**

(A) Volcano plot analysis showing number of genes (represented by dots) upregulated in fetal or adult V $\gamma$ 1<sup>+</sup> cells, compared with each other. Genes were considered significantly upregulated using empirical Bayes moderated t statistics (Table S1).

(B) Heatmap analysis showing select gene expression levels in fetal or adult V $\gamma$ 1<sup>+</sup> cells, relative to each other. Data are from one independent experiment. n = 2 replicates per group, with 8 mice pooled for each replicate for each group.

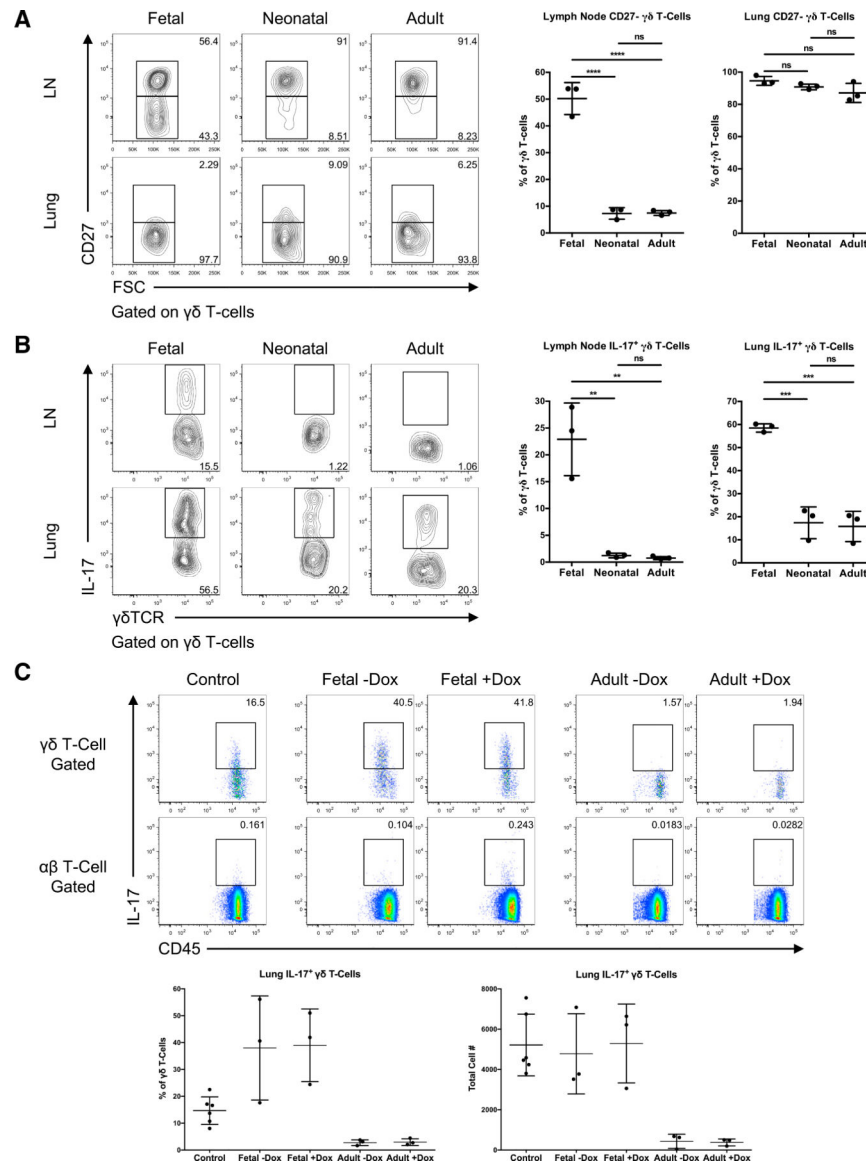


### Figure 3. Ontogenic timing influences $\gamma\delta$ T17 generation

(A) Flow cytometry analysis of CD27 expression by  $\gamma\delta$  T cells in lymph nodes and lung of fetal-, neonatal-, or adult-induced RBPJ<sup>ind</sup> mice (left); right panels show percentages.

(B) Flow cytometry analysis of IL-17 production by  $\gamma\delta$  T cells in lymph nodes and lung of mice as in (A) stimulated with PMA and ionomycin *in vitro* (left); right panels show percentages. Data are representative of three independent experiments. Data are presented as means  $\pm$  standard deviation of three independent experiments.  $n = 3$  mice per group. \*\* $p < 0.01$ , \*\*\* $p < 0.001$ , \*\*\*\* $p < 0.0001$  (one-way ANOVA).

(C) Flow cytometry analysis of IL-17 production by  $\gamma\delta$  T cells in lung of control, fetal-, or adult-induced RBPJ<sup>ind</sup> mice after TDM challenge (top); bottom panels show percentages and numbers. Data are representative of three independent experiments. Data are presented as means  $\pm$  standard deviation of three independent experiments.  $n = 6$  mice for control;  $n = 3$  mice per fetal- and adult-induced groups.

Statistical analyses between groups are found in Figure S2D.

Author Manuscript

Author Manuscript

Author Manuscript

Author Manuscript

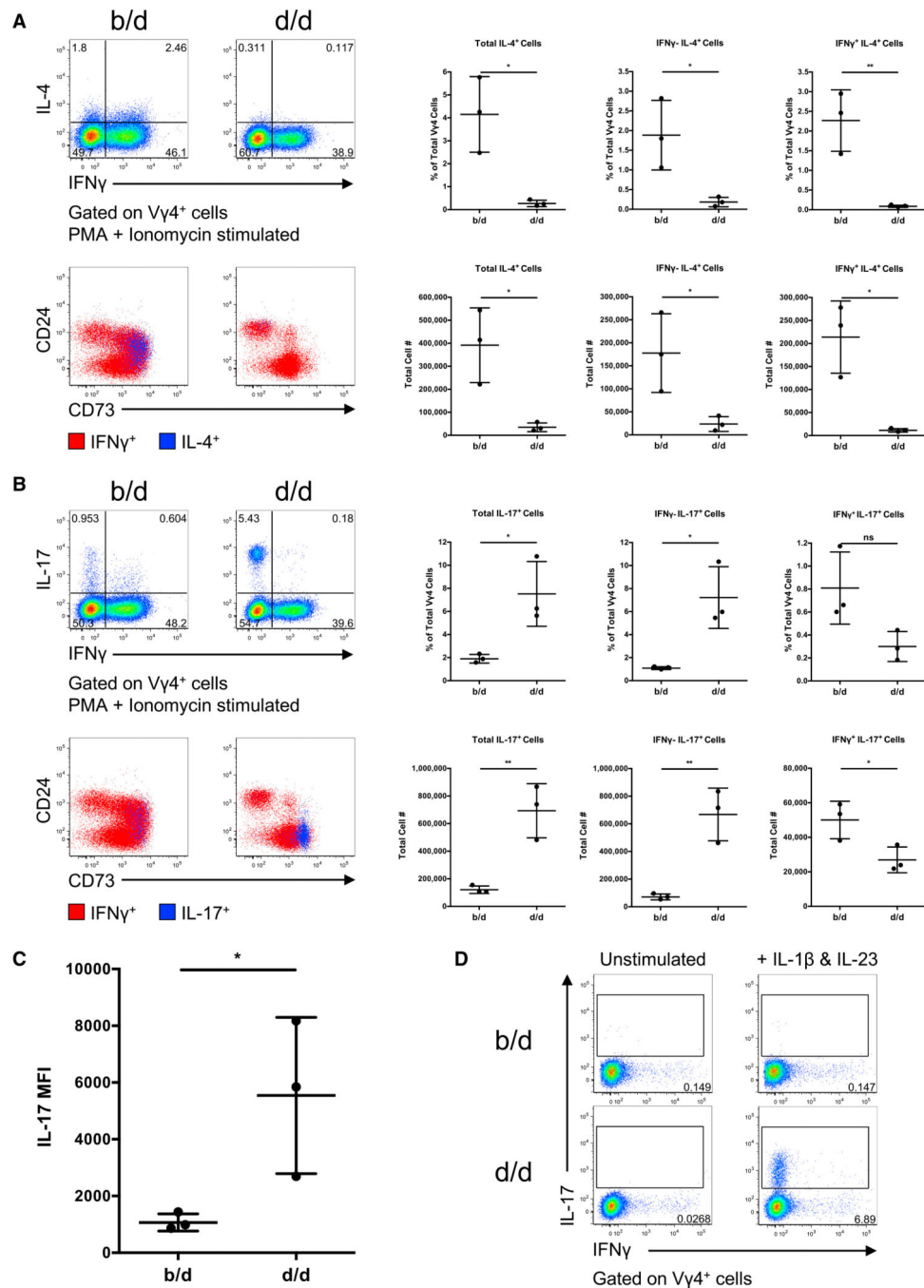


**Figure 4. TCR signaling influences  $\gamma\delta$  T cell functional differentiation**

(A) Flow cytometry analysis of IFN $\gamma$  and IL-4 production by thymic KN6 cells from b/d and d/d KN6<sup>tg</sup> mice stimulated with PMA and ionomycin *in vitro* (left); right panels show percentages and numbers.

(B) Flow cytometry analysis of IFN $\gamma$  and IL-17 production by thymic KN6 cells from mice and stimulated as in (A) (left); right panels show percentages and numbers.

(C) IL-17 MFI of thymic KN6 cells from mice and stimulated as in (A).

(D) Flow cytometry analysis of IL-17 production by thymic KN6 cells from mice as in (A) stimulated with IL-1 $\beta$

and IL-23 *in vitro*. Data are representative of three independent experiments. Data are presented as means  $\pm$  standard deviation of three independent experiments. n = 3 mice per group. \*p < 0.05, \*\*p < 0.01 (two-tailed unpaired t test).

Author Manuscript

Author Manuscript

Author Manuscript

Author Manuscript

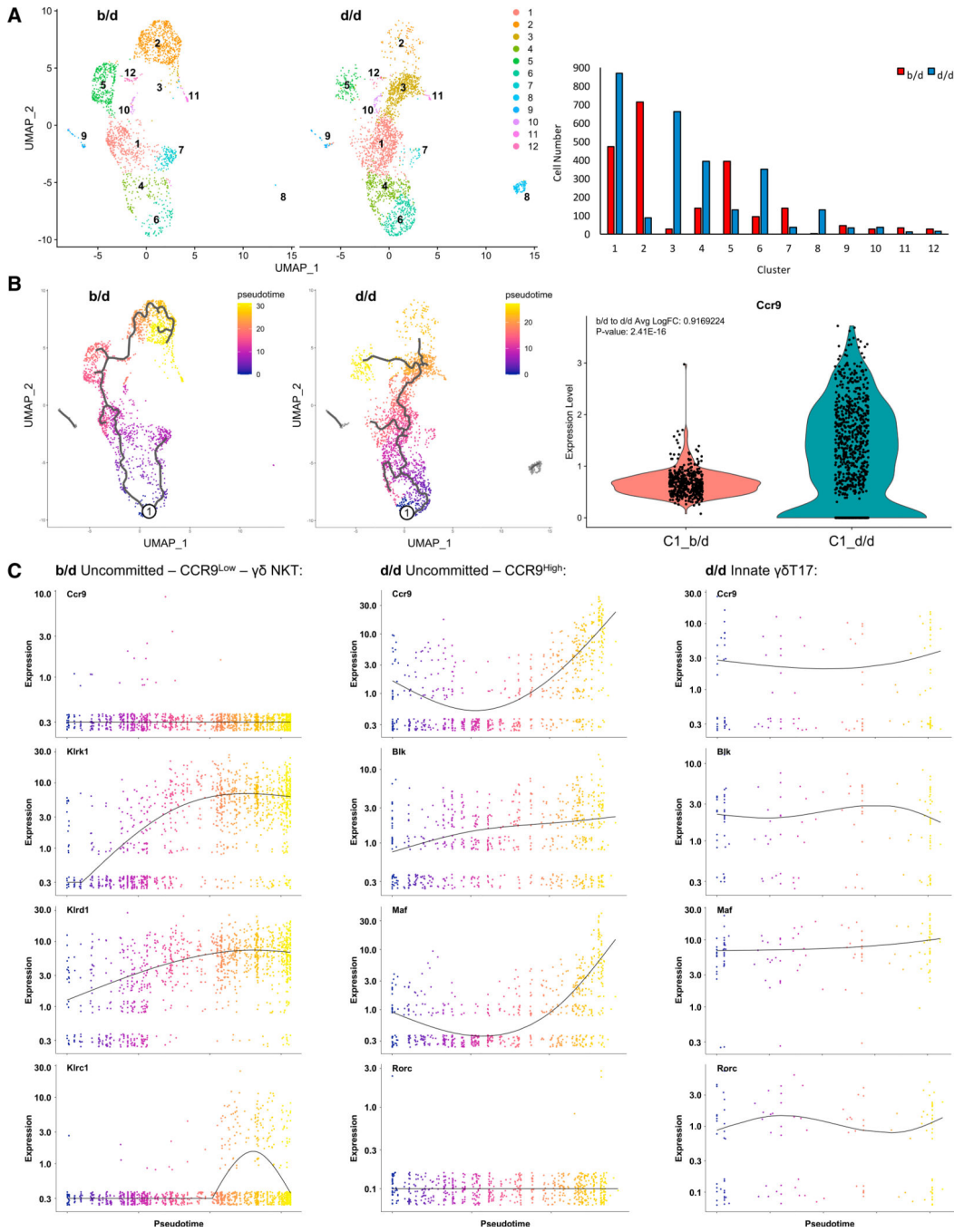


**Figure 5. Transcriptomic analysis of TCR signaling in  $\gamma\delta$  T cell functional differentiation**  
 (A) UMAP analysis of cell clusters 1–12 of thymic KN6 cells from b/d and d/d KN6<sup>tg</sup> mice (left). Cell clusters were defined by differential gene expression, which was determined by a Wilcoxon rank-sum test (Table S2). Cell cluster distribution of thymic KN6 cells from indicated mice (right). Statistical significance of cell cluster distribution was determined by a chi-square test (Table S3).

(B) Pseudotime analysis of cell trajectories starting from cluster 6 (left) and *Ccr9* expression in cluster 1 (right) of thymic KN6 cells from mice as in (A) (left). Statistical significance of *Ccr9* expression was determined by a Wilcoxon rank-sum test.

(C) Gene expression changes by b/d thymic KN6 cells from uncommitted cells (cluster 6) to CCR9<sup>low</sup> cells (cluster 1) to  $\gamma\delta$  NKT cells (cluster 2) (left). Gene expression change by d/d thymic KN6 cells from uncommitted cells (cluster 6) to CCR9<sup>high</sup> cells (cluster 1) to innate  $\gamma\delta$ T17 cells (cluster 8) (right). Data are from one independent experiment. n = 2,112 cells from 3 pooled mice for b/d; n = 2,753 cells from 3 pooled mice for d/d.



deviation of three independent experiments.  $n = 6$  mice per b/d group;  $n = 3$  mice per d/d group.  $*p < 0.05$ ,  $**p < 0.01$ ,  $***p < 0.001$  (two-tailed unpaired t test). (C) UMAP analysis of cell clusters 1–12 of thymic KN6 cells from b/d++ (Dox<sup>+8d+4d</sup>) and b/d+- (Dox<sup>+8d-4d</sup>) RBPJ<sup>ind</sup>KN6<sup>lg</sup> mice (left). Cell clusters were defined by differential gene expression, which was determined by a Wilcoxon rank-sum test (Table S4). Cell cluster distribution of thymic KN6 cells from indicated mice (right). Statistical significance of cell cluster distribution was determined by a chi-square test (Table S3). Data are from one independent experiment.  $n = 2,775$  cells from 5 pooled mice for b/d++;  $n = 3,065$  cells from 5 pooled mice for b/d+-.

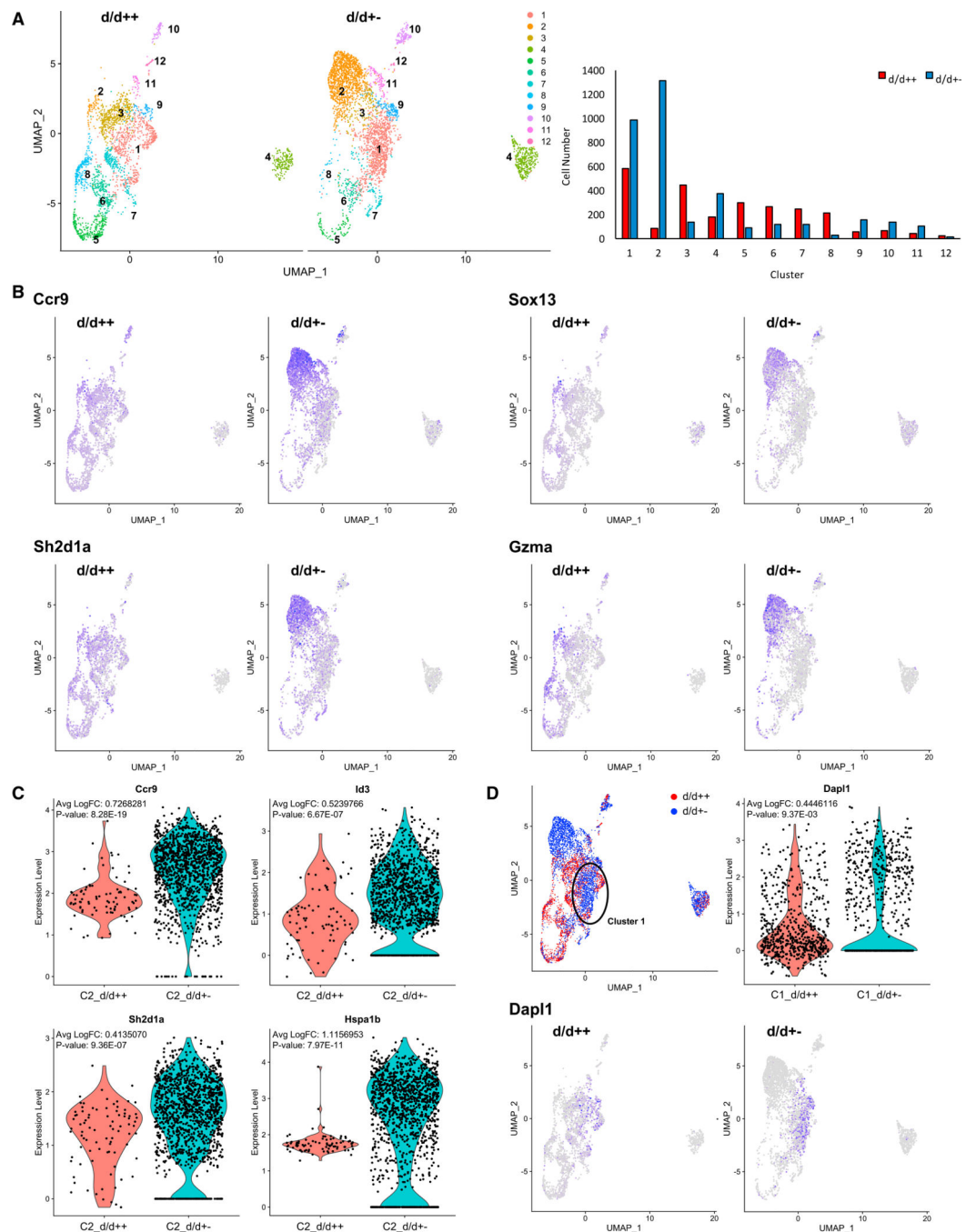


**Figure 7. Transcriptomic analysis of Notch signaling in  $\gamma\delta$  T cell functional differentiation with less strong TCR signals**

(A) UMAP analysis of cell clusters 1–12 of thymic KN6 cells from *d/d++* (Dox<sup>+8d+4d</sup>) and *d/d-* (Dox<sup>+8d-4d</sup>) RBPJ<sup>ind</sup>KN6<sup>tg</sup> mice (left). Cell clusters were defined by differential gene expression, which was determined by a Wilcoxon rank-sum test (Table S5). Cell cluster distribution of thymic KN6 cells from indicated mice (right). Statistical significance of cell cluster distribution was determined by a chi-square test (Table S3).

(B) UMAP analysis of cluster 2 enriched genes of thymic KN6 from mice as in (A).

(C) Indicated gene expression in cluster 2 of thymic KN6 cells from mice as in (A).

Statistical significance of gene expression was determined by a Wilcoxon rank-sum test. (D) *Dapl1* expression in cluster 1 (top) and UMAP analysis of *Dapl1* expression (bottom) of thymic KN6 cells from mice as in (A). Statistical significance of gene expression was determined by a Wilcoxon rank-sum test. Data are from one independent experiment. n = 2,505 cells from 3 pooled mice for d/d++; n = 3,568 cells from 3 pooled mice for d/d+/-.

## KEY RESOURCES TABLE

REAGENT or RESOURCE	SOURCE	IDENTIFIER
Antibodies		
PE anti-mouse CD44	BD Biosciences	553134
APC-Cy7 anti-mouse CD25	BD Biosciences	557658
PerCP-Cy5.5 anti-mouse $\gamma\delta$ TCR	BioLegend	118118
PE-Cy7 anti-mouse CD3	eBiosciences	25003182
APC anti-mouse V $\gamma$ 1	BioLegend	141108
APC anti-mouse V $\gamma$ 4	BioLegend	137708
FITC anti-mouse V $\gamma$ 4	BioLegend	137704
APC anti-mouse V $\gamma$ 5	BioLegend	137506
Purified anti-mouse V $\gamma$ 6	Michele Anderson Lab	manderso111@gmail.com
Purified anti-mouse V $\gamma$ 7	Pablo Pereira Lab	ppereira@pasteur.fr
AF700 anti-mouse CD45	BioLegend	103128
PE anti-mouse PLZF	BD Biosciences	564850
APC-Cy7 anti-mouse CD27	eBiosciences	47027182
APC anti-mouse IL-17	eBiosciences	17717781
APC anti-mouse IL-4	eBiosciences	17704182
PE anti-mouse IFN $\gamma$	BD Biosciences	554412
APC-Cy7 anti-mouse CD24	eBiosciences	47024282
PerCP-Cy5.5 anti-mouse CD73	BioLegend	127214
PE anti-mouse CD73	BioLegend	127206
PE anti-mouse CD4	eBiosciences	12004182
PE-Cy7 anti-mouse CD8	eBiosciences	25008182
Chemicals, peptides, and recombinant proteins		
Doxycycline	Sigma-Aldrich	D9891-100G
Brefeldin A	eBiosciences	00-4506-51
PMA	Sigma-Aldrich	P1585-1MG
Ionomycin	Sigma-Aldrich	I0634-1MG
IL-1 $\beta$	R&D Systems	401-ML-010
IL-23	R&D Systems	1887-ML-010
TDM	Sigma-Aldrich	T3034-1MG
Mineral oil	Sigma-Aldrich	M1180-500ML
Tween-80	Sigma-Aldrich	P4780-500ML
Critical commercial assays		
BD fixation/permeabilization solution kit	BD Biosciences	554714
BD LSR II	BD Biosciences	<a href="https://www.bd.com/resource.aspx?IDX=17868">https://www.bd.com/resource.aspx?IDX=17868</a>
BD FACSAria Fusion	BD Biosciences	<a href="https://wwwbdbiosciences.com/en-us/instruments/research-instruments/research-cell-sorters/facsaria-fusion">https://wwwbdbiosciences.com/en-us/instruments/research-instruments/research-cell-sorters/facsaria-fusion</a>

REAGENT or RESOURCE	SOURCE	IDENTIFIER
Takara SMARTer Stranded Total RNA-Seq Kit v3 – Pico Input Mammalian	Takara	<a href="https://www.takarabio.com/products/next-generation-sequencing/rna-seq/stranded-rna-seq-for-mammalian-samples/pico-input-strand-specific-total-rna-seq-for-mammalian-samples">https://www.takarabio.com/products/next-generation-sequencing/rna-seq/stranded-rna-seq-for-mammalian-samples/pico-input-strand-specific-total-rna-seq-for-mammalian-samples</a>
10x Genomics Chromium Controller v3	10x Genomics	<a href="https://www.10xgenomics.com/products/single-cell-gene-expression">https://www.10xgenomics.com/products/single-cell-gene-expression</a>
Illumina NovaSeq 6000	Illumina	<a href="https://www.illumina.com/systems/sequencing-platforms/novaseq.html">https://www.illumina.com/systems/sequencing-platforms/novaseq.html</a>
Experimental models: Organisms/strains		
RBPJ <sup>ind</sup> mice (males and females)	(Chen et al., 2019)	N/A
KN6 <sup>fl</sup> mice (males and females)	(Ito et al., 1990)	N/A
RBPJ <sup>ind</sup> KN6 <sup>fl</sup> mice (males and females)	Juan Carlos Zúñiga-Pflücker; Sunnybrook Research Institute	N/A
Software and algorithms		
FlowJo version 9.9.6	FlowJo	<a href="https://www.flowjo.com/solutions/flowjo/downloads">https://www.flowjo.com/solutions/flowjo/downloads</a>
Prism version 6	Graphpad	<a href="https://www.graphpad.com/scientific-software/prism/">https://www.graphpad.com/scientific-software/prism/</a>
HISAT2 version 2.1	Daehwan Kim Lab	<a href="https://daehwankimlab.github.io/hisat2/main/">https://daehwankimlab.github.io/hisat2/main/</a>
HTSeq version 0.1	Huber Group, EMBL Heidelberg	<a href="https://htseq.readthedocs.io/en/release_0.10.0/">https://htseq.readthedocs.io/en/release_0.10.0/</a>
Cell Ranger version 5.0	10x Genomics	<a href="https://support.10xgenomics.com/single-cell-gene-expression/software/pipelines/latest/what-is-cell-ranger">https://support.10xgenomics.com/single-cell-gene-expression/software/pipelines/latest/what-is-cell-ranger</a>
R version 3.6.3	R	<a href="https://www.r-project.org/">https://www.r-project.org/</a>
edgeR version 1	Yunchun Chen	<a href="https://f1000research.com/articles/5-1408/v1">https://f1000research.com/articles/5-1408/v1</a>
Seurat version 3	Rahul Satija Lab	<a href="https://satijalab.org/seurat/">https://satijalab.org/seurat/</a>
Monocle version 3	Cole Trapnell Lab	<a href="https://cole-trapnell-lab.github.io/monocle3/">https://cole-trapnell-lab.github.io/monocle3/</a>